

**LIGHTNING ANALYSIS OF A THUNDERSTORM ASSOCIATED
WITH LIGHTNING FLASHES IN MALACCA**



UNIVERSITI TEKNIKAL MALAYSIA MELAKA

**LIGHTNING ANALYSIS OF A THUNDERSTORM ASSOCIATED
WITH LIGHTNING FLASHES IN MALACCA**

TAN SHEA CHING

**This report is submitted in partial fulfilment of the requirements
for the degree of Bachelor of Electronic Engineering with Honours**

اونيورسيتي تيكنيكل مليسيا ملاك

**Faculty of Electronic and Computer Engineering
Universiti Teknikal Malaysia Melaka**

YEAR OF SUBMISSION: 20/21

DECLARATION

I declare that this report entitled “Lightning Analysis of a Thunderstorm Associated with Lightning Flashes in Malacca” is the result of my own work except for quotes as cited in the references.



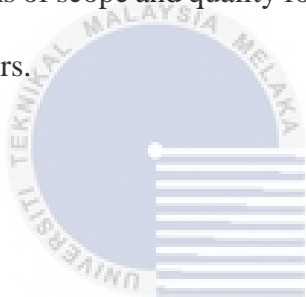
Signature :

Author : TAN SHEA CHING
.....

Date : 19/06/21
.....

APPROVAL

I hereby declare that I have read this thesis and in my opinion this thesis is sufficient in terms of scope and quality for the award of Bachelor of Electronic Engineering with Honours.



اونيورسيتي تيكنيكل مليسيا ملاك

Signature :

UNIVERSITI TEKNIKAL MALAYSIA MELAKA

Supervisor Name : DR. NORBAYAH BINTI YUSOP
.....

Date : **24 JUNE 2021**
.....

ABSTRACT

Lightning occurs when there are electrical imbalances between storm clouds and the ground, or inside the clouds themselves. Majority of lightning strikes within clouds. Generally, in Malaysia, positive lightning is extremely rare, and vast majority of CG lightning events are negative. On Tuesday, August 11, 2020, a thunderstorm rolled into the historic city of Malacca, causing considerable damage and injuring a number of students. Since the incident is happened so suddenly, the lightning analysis of a thunderstorm on August 11 have not been fully studied and discovered. Therefore, this paper presents the lightning analysis of a thunderstorm associated with lightning flashes in Malacca on 11 August 2020. There are 4 types of data used in this analysis by using electric field mill (EFM), fast electromagnetic field (FA) system, weather radar and world wide lightning location network (WWLLN). There are 1024 flashes detected with highest occurrence of lightning flashes is intracloud, IC (436 flashes) on 11 August 2020 in Malacca. Based on the EFM data, there are 2 storms occurred during 04:00:00 to 14:00:00. For the first storm, the highest electric field change is 0.75kV/m. FA data showed a total of 33 lightning flashes had detected with the highest number occurrence of flashes is 21 positive narrow bipolar event, NBE. The flash rate for the first storm is 28 flashes per hour. The maximum rainfall rate and reflectivity that detected by weather radar during the first storm is 8mm/h and 37dBZ respectively. The rainfall is moved from Klebang to Ayer Keroh after that to Alor Gajah. In addition, the highest electric field change in second storm is 9.8kV/m and there is a total of 980 lightning flashes detected by FA system with the highest number occurrence of flashes is 429 IC. The flash rate for the second storm is 320 flashes per hour. The radar data showed the highest rainfall rate and radar reflectivity is 50mm/h and 50dBZ respectively which happened in second storm. In second storm, the weather radar detected the rainfall moved from Masjid Tanah to whole area of Malacca. There are 338 lightning strikes detected by WWLLN during second storm but there is no any lightning strike detected during first storm. Majority of lightning strikes detected during the peak hour 10:00:00 to 10:59:59.

Keywords

Lightning, intracloud, narrow bipolar event, electric field change

ABSTRAK

Kilat berlaku apabila terdapat ketidakseimbangan elektrik antara awan ribut dan tanah, atau di dalam awan itu sendiri. Sebilangan besar kilat menyerang di awan. Secara amnya, di Malaysia, kilat positif sangat jarang berlaku, dan sebahagian besar kejadian kilat CG adalah negatif. Pada hari Selasa, 11 Ogos 2020, ribut petir melanda kota bersejarah Melaka, menyebabkan kerosakan yang besar dan mencederakan sejumlah pelajar. Oleh kerana kejadian itu berlaku secara tiba-tiba, analisis kilat ribut petir pada 11 Ogos belum dikaji dan ditemui sepenuhnya. Oleh itu, makalah ini menyajikan analisis kilat mengenai ribut petir yang berkaitan dengan kilat di Melaka pada 11 Ogos 2020. Terdapat 4 jenis data yang digunakan dalam analisis ini dengan menggunakan sensor kilang medan elektrik (EFM), sistem medan elektromagnetik cepat (FA), radar cuaca dan rangkaian lokasi kilat seluruh dunia (WWLLN). Terdapat 1024 kilatan yang dikesan dengan kejadian kilat tertinggi adalah intrakloud, IC (436 kilatan) pada 11 Ogos 2020 di Melaka. Berdasarkan data EFM, terdapat 2 ribut yang berlaku pada jam 04:00:00 hingga 14:00:00. Untuk ribut pertama, perubahan medan elektrik tertinggi ialah $0.75\text{kV} / \text{m}$. Data FA menunjukkan sejumlah 33 kilatan kilat telah dikesan dengan jumlah kilatan tertinggi adalah 21 peristiwa bipolar sempit positif, NBE. Kadar kilat untuk ribut pertama adalah 28 kilatan sejam. Kadar hujan maksimum dan pantulan yang dikesan oleh radar cuaca semasa ribut pertama masing-masing adalah $8\text{mm} / \text{j}$ dan 37dBZ . Hujan dipindahkan dari Klebang ke Ayer Keroh selepas itu ke Alor Gajah. Di samping itu, perubahan medan elektrik tertinggi dalam ribut kedua ialah $9.8\text{kV} / \text{m}$ dan terdapat sejumlah 980 kilat kilat yang dikesan oleh sistem FA dengan jumlah kilat tertinggi adalah 429 IC. Kadar kilat untuk ribut kedua ialah 320 kilatan sejam. Data radar menunjukkan kadar hujan tertinggi dan pantulan radar masing-masing $50\text{mm} / \text{j}$ dan 50dBZ yang berlaku dalam ribut kedua. Dalam ribut kedua, radar cuaca mengesan hujan berpindah dari Masjid Tanah ke seluruh wilayah Melaka. Terdapat 338 serangan kilat yang dikesan oleh WWLLN semasa ribut kedua tetapi tidak ada serangan kilat yang dikesan semasa ribut pertama. Sebilangan besar serangan kilat dikesan pada waktu puncak 10:00:00 hingga 10:59:59.

Kata kunci

Kilat, intrakloud, peristiwa bipolar sempit, perubahan medan elektrik

ACKNOWLEDGEMENTS

This final year project report in BENU 4984 Projek Sarjana Muda Bhg II may not be finished with a thorough target without full support, assisting, and commitment, as well as participation from all persons and parties concerned, whether direct or indirect.

First and foremost, I would like to thank to my supervisor, Dr Norbayah binti Yusop, senior lecturer of Faculty of Electronic and Computer Engineering (FKEKK), University Teknikal Malaysia Melaka (UTeM) for the guidance and give a lot of helps when I get in troubles doing this project. She also gives me full support, encouragement, contribution of idea, spending time to discuss with me about the project, and very patient to answer all my questions. Besides that, special thanks to Dr. Mohd Riduan bin Ahmad who also gives a lot of helps, guidance and impart knowledges of related field. He also spending time to discuss the project with me despite his busy schedules.

Moreover, I would like to express my gratitude towards my fellow friends for giving me a lot of helps so that I can complete the project on time. I also would like to thank my family members who gave me ethical support and advice while doing this project.

Lastly, not forgetting for those people who are involved direct and indirect ways. Thanks to everyone.

TABLE OF CONTENTS

| | |
|--|----------------|
| Declaration | |
| Approval | |
| Dedication | |
| Abstract | i |
| Abstrak | ii |
| Acknowledgement | iii |
| Table of Contents | iv-vii |
| List of Figures | viii-xi |
| List of Tables | xii |
| List of Symbols and Abbreviations | xiii |
| CHAPTER 1 INTRODUCTION | 1-4 |
| 1.1 BACKGROUND RESEARCH | 1-2 |
| 1.2 PROBLEM STATEMENT | 2 |
| 1.3 OBJECTIVES | 3 |
| 1.4 SCOPE OF WORK | 3 |
| 1.5 THESIS OUTLINE | 4 |



| | |
|---|--------------|
| CHAPTER 2 LITERATURE REVIEW | 5-27 |
| 2.1 INTRODUCTION | 5 |
| 2.2 LITERATURE REVIEW | 5-9 |
| 2.3 TYPE OF LIGHTNING FLASHES | 10-13 |
| 2.3.1 CLOUD TO GROUND (CG) LIGHTNING | 10-11 |
| 2.3.2 INTRACLOUD (IC) | 12-13 |
| 2.4 UNUSUAL FORMS OF LIGHTNING FLASHES | 14-17 |
| 2.4.1 FORKED LIGHTNING | 14-15 |
| 2.4.2 LIGHTNING WITHOUT THUNDER | 16 |
| 2.4.3 BALL LIGHTNING | 17 |
| 2.5 MECHANISM OF LIGHTNING FLASHES | 18-19 |
| 2.5.1 MECHANISM OF UPWARD INITIATE LIGHTNING FLASHES | 18 |
| 2.5.2 MECHANISM OF POSITIVE GROUND FLASHES AND THEIR MAIN DIFFERENCE WITH NEGATIVE GROUND FLASHES | 19 |
| 2.6 CLASSIFICATION OF LIGHTNINGS BY TYPES AND POLARITIES | 20-22 |
| 2.7 LIGHTNING STRIKE | 23 |
| 2.8 LIGHTNING DISCHARGE | 24-27 |
| 2.8.1 PRELIMINARY BREAKDOWN PULSE | 24-25 |
| 2.8.2 STEPPED LEADER | 26-27 |
| CHAPTER 3 METHODOLOGY | 28-43 |

| | | |
|---|--|--------------|
| 3.1 | INTRODUCTION | 28 |
| 3.2 | DATA COLLECTION AND TOOL | 28-38 |
| 3.2.1 | ELECTRIC FIELD MILL (EFM) | 28-31 |
| 3.2.2 | FAST ELECTROMAGNETIC FIELD ANTENNA SYSTEM (FA) | 32-33 |
| 3.2.3 | WEATHER RADAR | 34-36 |
| 3.2.4 | WORLD WIDE LIGHTNING LOCATION NETWORK (WWLLN) | 37-38 |
| 3.3 | DATA PROCESSING | 39-43 |
| CHAPTER 4 RESULTS AND DISCUSSION | | 44-64 |
| 4.1 | INTRODUCTION | 44 |
| 4.2 | COMPARISON BETWEEN EFM, FA SYSTEM, WEATHER RADAR AND WWLLN | 44-64 |
| 4.2.1 | OCCILATION OF AN ELECTRIC FIELD | 44-45 |
| 4.2.2 | ANALYSIS OF TYPE OF LIGHTNING FLASHES | 46-48 |
| 4.2.3 | ANALYSIS OF RADAR DATA | 49-53 |
| 4.2.4 | WORLD WIDE LIGHTNING LOCATION NETWORK (WWLLN) DATA | 54-56 |
| 4.2.5 | CORRELATION BETWEEN ELECTRIC FIELD, LIGHTNING FLASHES, RAINFALL RATE AND WWLLN | 57-64 |
| CHAPTER 5 CONCLUSION AND FUTURE WORK | | 65-66 |
| 5.1 | CONCLUSION | 65 |

5.2 RECOMMENDATIONS FOR FUTURE WORK

66

REFERENCES

67-70



LIST OF FIGURES

| | |
|---|----|
| Figure 2.1: Schematic description of lightning detection system | 9 |
| Figure 2.2: Negative cloud to ground lightning (-CG) | 11 |
| Figure 2.3: Positive cloud to ground lightning (+CG) | 11 |
| Figure 2.4: Intracloud | 13 |
| Figure 2.5: Cloud to air lightning | 13 |
| Figure 2.6: Cloud to cloud lightning | 13 |
| Figure 2.7: To the naked eye, forked lightning appears | 14 |
| Figure 2.8: Process of return stroke for forked lightning | 15 |
| Figure 2.9: From a location below the thundercloud, two strokes of the same flash (separated in time by the amount $T_2 - T_1$) follow two different routes to ground (point marked A) | 15 |
| Figure 2.10: The occurrence of lightning without thunder. | 16 |
| Figure 2.11: The basic characteristics of an upward initiated lightning flash | 18 |
| Figure 2.12: Electrostatic field changes produced by negative CG | 20 |
| Figure 2.13: Fast electric field record of negative CG | 20 |
| Figure 2.14: Electrostatic field changes produced by positive CG | 21 |
| Figure 2.15: Fast electric field record of positive CG | 21 |
| Figure 2.16: Electrostatic field changes of opposite polarity produced by inverted-polarity IC flash | 21 |
| Figure 2.17: Fast electric field record of inverted-polarity IC flash | 22 |

| | |
|---|----|
| Figure 2.18: Negative NBE | 22 |
| Figure 2.19: Positive NBE | 22 |
| Figure 2.20 (a): 3 return strokes of lightning flash that captured by FA system at 10-20km | 25 |
| Figure 2.20 (b): high-frequency (HF) radiation at 3 MHz | 25 |
| Figure 2.21: A clear preliminary breakdown pulse train, intermediate, and tiered ladder can be seen in this example of negative cloud-to-ground lightning | 25 |
| Figure 2.22: Mechanism of lightning initiation: (a) stepped leader formation; (b) initiation of an upward leader; (c) return stroke | 27 |
| Figure 2.23: Charge of stepped leaders | 27 |
| Figure 3.1: Electric field mill (EFM) sensor | 30 |
| Figure 3.2: Electric field monitor software shows all clear status | 30 |
| Figure 3.3: Electric field monitor software shows lightning and high field alarm active | 31 |
| Figure 3.4: Schematic of a shutter-type EFM | 31 |
| Figure 3.5: Setup of fast and slow electromagnetic fields antenna system | 33 |
| Figure 3.6: Fast and slow electromagnetic field antenna system that located at Universiti Teknikal Malaysia Melaka (UTeM), Malacca, Malaysia (2.314077° N, 102.318282° E) | 33 |
| Figure 3.7: Radar Malaysia map | 36 |
| Figure 3.8: The meanings of radar color | 36 |
| Figure 3.9: Example of WWLLN | 38 |
| Figure 3.10: Flow chart of the research | 40 |
| Figure 3.11: Representation of each color lines in Picoscope 6 software | 41 |

| | |
|---|----|
| Figure 3.12: Example waveform that captured by FA system at 04:02:18 on 11 August 2020 in Malacca | 41 |
| Figure 3.13: Example waveform that captured by FA system at 05:46:40 on 11 August 2020 in Malacca | 42 |
| Figure 3.14: Example waveform that captured by FA system at 05:47:28 on 11 August 2020 in Malacca | 42 |
| Figure 3.15: Example of radar data at 05:10:08 on 11 August 2020 | 43 |
| Figure 3.16: Example code for WWLLN data | 43 |
| Figure 4.1: Electric field at the ground on 11 August 2020 | 45 |
| Figure 4.2: Type of lightning flashes detected by FA system on 11 August 2020 in Malacca | 47 |
| Figure 4.3: Number of return strokes detected by FA system on 11 August 2020 in Malacca | 47 |
| Figure 4.4: The expended view of fast field signal at 10:06:48 | 48 |
| Figure 4.5: Evolution of flash rate per 10 minutes on 11 August 2020 in Malacca | 48 |
| Figure 4.6: Rainfall rate recorded by weather radar on 11 August 2020 | 50 |
| Figure 4.7: Radar reflectivity recorded by weather radar on 11 August 2020 | 50 |
| Figure 4.8: The location of lightning strike detected by WWLLN | 55 |
| Figure 4.9: Energy of lightning strike detected by WWLLN on 11 August 2020 in Malacca | 55 |
| Figure 4.10: Evolution of strike rate on 11 August 2020 on Malacca | 56 |
| Figure 4.10: Type of lightning flashes detected by FA system from 05:00:00 to 06:59:59 (first storm) | 59 |
| Figure 4.11: Type of lightning flashes detected by FA system from 07:00:00 to 14:00:00 (second storm) | 59 |

- Figure 4.12: Type of lightning flashes before and after 10:48:22 (highest electric field) 60
- Figure 4.13(a): Location of lightning strike detected by WWLLN 60
- Figure 4.13(b): Active region for highest reflectivity detected by weather radar 60



LIST OF TABLES

| | |
|---|----|
| Table 2.1: Statistical analysis of yearly flash count includes AM, GM, Min and Max values all data obtained between 2004 and 2011 | 9 |
| Table 3.1: The Z-R relationships | 36 |
| Table 4.1: Maximum rainfall rate detected by weather radar on 11 August 2020 in Malacca | 51 |
| Table 4.2: Number of lightning strike detected by WWLLN on 11 August 2020 | 56 |
| Table 4.3: Comparison between analysis obtained by EFM, weather radar and WWLLN | 61 |
| Table 4.4: Summary of first and second storm on 11 August 2020 in Malacca | 64 |



LIST OF SYMBOLS AND ABBREVIATIONS

| | |
|-------|---|
| CG | : Cloud-to-ground |
| IC | : Intracloud |
| NBE | : Narrow bipolar event |
| PBP | : Preliminary breakdown pulse |
| EFM | : Electric field mill |
| FA | : Fast electromagnetic field antenna system |
| WWLLN | : World Wide Lightning Location Network |
| MMD | : Malaysia Meteorological Department |
| CAPPI | : Constant Altitude Plan Position Indicator |
| VLF | : Very low frequency |
| VHF | : Very high frequency |
| OS | : Observation station |
| NWS | : National Weather Service |

CHAPTER 1

INTRODUCTION

1.1 BACKGROUND RESEARCH

This project is more focus on analyse the lightning flashes which causing the thunderstorm happens in Malacca. On Tuesday (11 August 2020), a thunderstorm happened at Malacca, causing serious damage and injuring a number of students. The worst-affected locations were Malim, Batu Berendam, Taman Merdeka Permai, and Klebang. Several cars were also damaged, and a vernacular primary school's roof was pulled off, hurting several students. Since the incident was happened so suddenly, the lightning analysis of a thunderstorm associated with lightning flashes on August 11 have not been fully studied and discovered.

Moreover, a thunderstorm produces lightning, which is a dazzling flash of electricity. It is an electrical discharge caused by imbalance between storm clouds and the earth, or within the clouds themselves. The majority of lightning happened within clouds. There are several types of lightning such as cloud-to-ground (CG) which consists positive CG (+CG) and negative CG (-CG), intracloud (IC), narrow bipolar event (NBE) which also consists positive NBE (+NBE) and negative NBE (-NBE). Most of CG lightning events occurred in Malaysia is negative CG, the present of positive CG is approximately 10% of total number of CG lightning events. Between the all type of lightning, cloud-to-ground lightning is the most dangerous type of lightning. Most cloud-to-ground lightning strikes come from the negatively charged bottom of the cloud traveling to the positively charged ground below. While intercloud lightning is less common. It is when a lightning strike occurs when there are positive and negative charges within different clouds and the strike travels in the air between them.

In this research, the data involved is collected from electric field mill (EFM), fast electric field antenna (FA) system, weather radar and world wide lightning location network

(WWLLN). Based on the lightning data collected, process and analyse the data to differentiate the type and characteristics of lightning flashes that caused the occurrence of thunderstorms on 11 August 2020 in Malacca and the correlation between electric field, lightning flashes, rainfall rate and WWLLN data. EFM is used to measure the static atmospheric electric field at the location of the instrument. FA system is chosen because FA system is a well-known and accurate lightning measurement. The FA data is used to classify the types of lightning flashes such as CG, IC and NBE. Weather radar is used to estimate the rainfall rate by using the colour gauge. Then, WWLLN is used to detect the coordinate and number of lightning strikes.

In addition, the area of observation is set at Malacca (latitude: $2^{\circ}11'45.6''$ N, longitude: $102^{\circ}14'25.8''$ E). The duration for data collection is 10 hours which is from 4am to 2pm. By having the analysis of all data obtained, it can be used as an indicator to predict the thunderstorm event to be occur in the future.

1.2 PROBLEM STATEMENT

On Tuesday (11 August 2020), a thunderstorm happened at Malacca, causing serious damage and injuring a number of students. The worst-affected locations were Malim, Batu Berendam, Taman Merdeka Permai, and Klebang. Several cars were also damaged, and a vernacular primary school's roof was pulled off, hurting several students.

Since the incident is happened so suddenly, the research about the lightning analysis of a thunderstorm such as the types and characteristics of the lightning flashes, and which type of lightning flashes caused thunderstorm happened had not been fully studied and discovered.

Besides that, correlation between electric field, lightning flashes, rainfall rate and WWLLN data that detected on 11 August 2020 in Malacca also had not been analysed.

1.3 OBJECTIVES

The main purpose in this research is to study the type and characteristics of lightning flashes and which type of lightning caused thunderstorm that occurred on 11 August 2020 in Malacca. There are 2 objectives such as

- i. To classify the types of lightning flashes.
- ii. To analyse the correlation between the electric field, lightning flashes, rainfall rate and WWLLN data.

1.4 SCOPE OF WORK

The research about the analysis of lightning flashes during thunderstorm event in Malacca, type of lightning, characteristics of each type of lightning are carried out. The data that involved in this research is FA data, EFM data, radar data and WWLLN data. For the duration to collect the data is 10 hours (11 August 2020, from 4am until 2pm). The area of observation is set at Malacca (latitude: $2^{\circ}11'45.6''$ N, longitude: $102^{\circ}14'25.8''$ E). Besides that, the research about the method to study the lightning data, radar data and WWLLN data that collected by EFM, FA system, weather radar and WWLLN are studied. The lightning data is collected by using EFM, FA system, and WWLLN while the radar data is obtained from Malaysia Meteorological Department (MMD). Both the EFM and FA system are installed at Universiti Teknikal Malaysia Melaka (UTeM). Moreover, the observation station for weather radar is also located at UTeM. Additionally, the electric field change is examined by using the graph that obtained from MATLAB software. The characteristics and types of the lightning flashes are examined and analyzed. The classification of type of lightning is carried out by observing the waveform of each lightning data by using Picoscope 6 software. For radar data, rainfall rate are estimated based on the color gauge. The coordinate and number of lightning strike is detected by WWLLN. Next, the correlation is made based on the electric field, lightning flashes, rainfall rate and WWLLN data. Other than that, several graphs, bar chart and tables are constructed based on the data that collected from different system.

1.5 THESIS OUTLINE

The body of the contents of this project is categorized into five chapters. These chapters include introduction, literature review, methodology, results, analysis, discussion, and conclusion.

The first chapter is introduction. It briefly describes the incident that happen in Malacca on 11 August 2020 and background studies lightning analysis. Next, the problem statement, objectives, and scope of work of this project are listed out in this chapter.

The second chapter is literature review. This chapter provide the reader with a more detail about the lightning analysis such as type of lightning, characteristics of each type of lightning, mechanism of lightning flash, lightning strike, lightning strike and so on.

The third chapter is methodology. This chapter consist of the overview of each instrument that used in this research, and the methods to study and analyze the data obtained. Furthermore, the key task list and the project flow chart are prepared to plan the task and the duration of doing it.

The fourth chapter is results and discussion. This chapter presents about the results obtained from the EFM, FA system, weather radar and WWLLN. Based on the results, analyze the electric field change, type of lightning flashes, rainfall rate, coordinate and number of lightning strike detected. Several graphs, bar charts, and tables are displayed in this chapter also. After that, correlate electric field, lightning flashes, rainfall rate and WWLLN data and discuss about it.

The last chapter is conclusion and future work. This chapter has concluded all the analysis at chapter fourth and there are some suggestions to improve the weaknesses in this project.

CHAPTER 2

LITERATURE REVIEW

2.1 INTRODUCTION

This chapter presents about the general overview of lightning, previous work from other researcher, types of lightning flashes, unusual form of lightning flashes, mechanism of lightning flashes, classification of lightning by types and polarity, lightning strike, and lightning discharge.

2.2 LITERATURE REVIEW

The public and utility corporations in Malaysia are concerned about the frequent occurrence of lightning-related accidents. The rate of lightning fatalities is estimated to be ten times higher than in the United States. The smart public will be better able to make educated judgments about personal safety and asset protection if they have a general understanding of the dispersion of lightning flashes. For more than three decades, the Malaysian Meteorological Service (MMS) has been collecting statistics on thunderstorm day level. For nearly a decade, a private utility corporation has been collecting data on lightning flash density using a lightning detection network [1].

Using the lightning reports of surface observers and the first generation of weather radar, scientists attempted to explain the relationship between the lightning rate and the vertical structure of radar reflectivity in thunderstorms more than half a century ago. Using RPFs with at least one flash, the relationships between flash rates and radar echo top temperatures, regions and volumes of radar reflectivity, and ice water contents in the mixed phase zone are investigated. When supercooled liquid water is present, good correlations between radar

reflectivity at altitudes and lightning flash rate can be explained by the non-inductive charging theory, which states that collisions between radar sensitive precipitation ice particles and smaller cloud ice particles can separate the electric charge. The ice particles holding opposite charges could concentrate in different parts of the storm due to varying terminal velocities, resulting in intense electric fields and lightning [2].

Recent studies by Norbayah Yusop, Mohd Riduan Ahmad et.al, a seasonal analysis of cloud-to-ground (CG) lightning flash activity was conducted in the Western Antarctica using a lightning detector sensor installed at the Carlini Base station. Between February and December 2017, data from the detecting system was evaluated. Within a 1000 km radius of the station, the sensor observed three common places and areas of composite active thunderstorms (labelled storm regions A, B, and C). There were a total of 2,019,923 flashes observed, with 43.01 percent being positive CG flashes and 56.99 percent being negative CG flashes. According to the study, more than 96 percent of the CG flashes which both positive and negative CG were produced during the summer and fall seasons, compared to less than 4% during the winter and spring seasons. Storm region B produced the majority of the observed lightning strokes which more than 85% in the center area around the station, with storm regions A and C generating fewer than 15% in the ocean areas over the Amundsen/Bellingshausen Sea and the Weddell Sea [3].

According to research done by Hwee Geem Chan and Amir Izzani bin Mohamed, analysis from this study found that a high number of lightning occur during dry season compares to rainy season. This is in contrast to popular thinking in Malaysia, which holds that lightning only happens on rainy days. It is also known that +CG lightning contributes for around 20% of all lightning, with the remainder consisting of CG lightning events. +CG lightning will be discussed both during the day and at night. The direction of most +CG lightning will be determined as a result of this, then it will be used as a guide to examine TLEs subsequently [4].

Based on the recent studies by Norbayah Yusop, Mohd Riduan Ahmad et.al, From a collection of storm days between February and July 2017, three storm days for each month that within a 1,000 km radius of the LD sensor were chosen, each having three composite active thunderstorms which labelled as Storm area A, B, and C. From these 54 thunderstorms, a total

of 355,899 flashes were observed, with 156,190 Positive CG and 199,709 negative CG flashes. Positive CG flash counts accounted for roughly 43.9 percent of all observed CG flashes. Majority of positive CG flashes which more than 80% had only one or two strokes, with a maximum of five. The average multiplicity and maximum multiple strokes for negative CG flashes were 1.2 and 16 respectively. Majority of CG flashes were observed in the summer and fall. Even during the winter, positive CG flashes were common in Western Antarctic storms. The ratio of positive CG to negative CG flashes had a mean, median, and range of 0.7, 0.718, and 0.217–1.279 respectively [5].

The recent studies by Mohd Riduan Ahmad, Dinesh Periannan Muhammad Haziq Mohammad Sabri et.al found that a total of 49 positive NBEs (+NBEs) were detected from the storm. According to emission heights and radar reflectivity data, the NBE activity can be separated into two stages. The first stage (or S1) lasted barely 6 minutes and produced 20 NBEs, starting with the first identified NBE (41 percent). The emission heights ranged from 12.0 to 16.7 kilometers. The storm achieved maximum levels of 55 dBZ within the period S1 according to radar reflectivity data. On the other hand, the second stage (S2), lasted 32 minutes and yielded 29 NBEs (59 percent). The emission heights were lower which ranging between 8.5 and 13.7 kilometers. The storm attained maximum levels of 50 dBZ within the timeframe S2 according to radar reflectivity data [6].

Based on the recent studies by Chin-Leong Wooi, Zulkurnain Abdul-Malek et.al, during the monsoon season in the Malaysia state of Johor, 104 negative lightning flashes with 277 negative return strokes were reported within 10–100 kilometers of the measuring station. Multiple strokes account for 73 percent of the recorded flashes with an average multiplicity of 2.6 strokes per flash. The arithmetic mean (AM) of the initial peak electric field and the AM of the initial peak electric field derivative for first return strokes are 21.8 V/m and 11.3 V/m/ms respectively. For the first return strokes, the first peaks of the electric field and its derivative are bigger than those for successive return strokes. Due to a shortage of statistical data in the tropical region, particularly in Malaysia, this research investigates the parameters of the electric field generated by negative lightning. The features of negative lightning should be explored further in order to improve lightning locating systems or lightning protection. These explained Malaysian-based characteristics can potentially be used to construct a return stroke model in the future [7].

The recent studies by C.L.Wooi, Zulkarnain Malek et.al showed that in Peninsular Malaysia, approximately a million flashes were reported between 2004 and 2011. Lightning flashes can occur either within the cloud (in-cloud flashes) or from the cloud to the ground (cloud-to-ground flashes. Cloud-to-ground lightning can be classified as either negative or positive return stroke, depending on the polarity of the starting charges within the cloud. For the years 2004 to 2011, the number of lightning flashes in Malaysia ranged from 684,594 to 2,853,162 flashes with an average of 1,549,085 flashes. Positive lightning contributes for only 14 to 31 percent of overall cloud-to-ground lightning activity in Malaysia. Positive lightning makes for 17.74 percent of total cloud-to-ground lightning activity in Malaysia. When compared to worldwide cloud-to-ground lightning, this figure is slightly higher which is approximate to 10 percent [8].

The recent studies by Chin-Leong Wooi, Zulkarnain Malek et.al found that the PBP for positive cloud-to-ground (+CG) lightning is considerably more complex than for –CG lightning since only negative PBP trains are normally present in –CG lightning. Based on the initial polarity of the 21 positive flashes studied, four types of PBP trains were discovered. Negative PBP accounts for 20% of the total, whereas positive PBP accounts for 15%, PBP with polarity reversal accounts for 10%, and PBP with irregular polarity accounts for 15%. The remaining 40% of flashes do not contain any PBP. The observed variances in cloud discharge processes which including the forms of PBP could be due to the effect of geographical area [9].

Based on the studies by Behnam Salimi, Kamyar Mehranzamir and Zulkarnain Abdul-Malek, the properties of broadband electric fields produced by cloud-to-ground lightning discharges in Malaysia's south are investigated. A total of 130 cloud-to-ground lightning flashes were studied from three separate thunderstorm events which each lasting around 4 to 5 hours. The time duration of the preliminary breakdown pulse train, time interval between preliminary breakdowns and return stroke, multiplicity of stroke, and percentages of single stroke only were all statistically analyzed. The BIL model is also used to describe the patterns of lightning signatures [10].

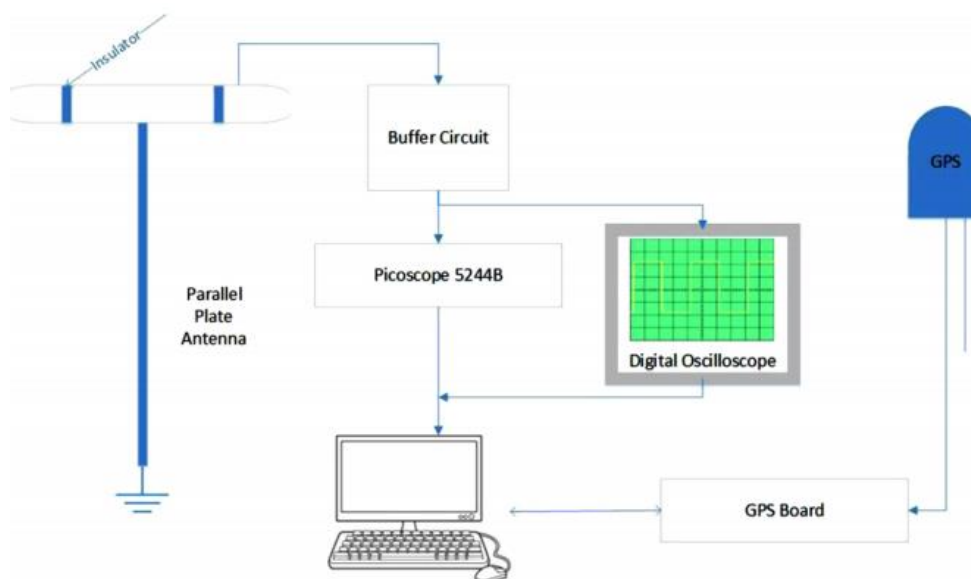


Figure 2.1: Schematic description of lightning detection system [10].

Table 2.1: Statistical analysis of yearly flash count includes AM, GM, Min and Max values all data obtained between 2004 and 2011 [8].

| | Positive Return Strokes | Negative Return Strokes | Total Return Strokes |
|-----|----------------------------|----------------------------|----------------------|
| AM | 290482 | 1258603 | 1549086 |
| GM | 232474 | 1116937 | 1361291 |
| Min | 108398 | 561367 | 684594 |
| Max | 843089 | 2448549 | 2853162 |
| SD | 242204 | 663445 | 846636 |

2.3 TYPE OF LIGHTNING FLASHES

Majority of lightning originates inside a thunderstorm and travels through the cloud. It can then either stay in the cloud or move through the open air until it reaches the ground. Individual storms may have more or fewer flashes reaching the ground, but there are typically 5 to 10 times as many flashes that remain in the cloud as there are flashes that travel to the ground [11].

2.3.1 CLOUD TO GROUND (CG) LIGHTNING

In CG lightning, a negative charge channel termed a stepped leader will zigzags downward in a "forked" pattern, hence the name "forked lightning." This stepped leader is imperceptible to the naked eye and travels to the ground in a microsecond [12]. A negative stepped leader travels downward into the cloud, followed by an upward moving return stroke in the more frequent cloud-to-ground flash. As a result of the flash's overall effect of lowering negative charge from the cloud to the ground, it's often referred to as a negative CG (-CG). A positive CG (+CG) is a positive charge that is lowered to ground by a downward travelling positive leader followed by an upward return stroke [13].

Besides that, the presence of -CGs is more common than the presence of +CGs. -CGs strikes are visually and photographically identifiable by their unique downward branching. -CGs are frequently composed of numerous return strokes which are extra current pulses that illuminate the channel repeatedly. The first return stroke of a -CG is usually the only branching one; subsequent return strokes normally do not illuminate the branches again [13].

Moreover, +CGs are the rarer of the two. A downward moving and positively charged stepped leader initiates CG flashes which is followed by an upward return stroke that lowers the positive charge to ground [8]. +CGs is made up of a single return stroke that is usually exceptionally intense and strong in comparison to other lightning activity in a storm. Thunder from a +CG is extremely loud, often sounding like a succession of deep, low-frequency sonic booms [13].



Figure 2.2: Negative cloud to ground lightning (-CG) [13].



Figure 2.3: Positive cloud to ground lightning (+CG) [13].

2.3.2 INTRACLOUD (IC)

The most common type of discharge is intracloud which refers to lightning that occurs within a single storm cloud and jumps between distinct charge zones [12]. Inside the cloud, all or part of the real channel may be obscured and an observer on the ground may or may not be able to see it [13].

Narrow bipolar pulses (NBPs) are a different category of intra-cloud (IC) flash that produces electric fields [14]. Narrow bipolar events (NBEs) are a rare and poorly understood type of breakdown that can occur as the initial event of an intracloud (IC) lightning flash or in isolation from other storm discharges [15].

The National Weather Service (NWS) defines cloud-to-air lightning as "lightning that occurs when the air around a positively charged cloud top reaches out to the negatively charged air surrounding it." In other words, these lightning strikes are the result of an attraction between oppositely charged clouds and air that never reaches the ground. However, most of the time the positive charge accumulates on top of a storm cloud and is attracted to a nearby negative charge [16].

Cloud to cloud lightning occurs when one cloud has a predominantly negative charge and another has a predominantly positive charge that leading the two to attract. According to the NSSL, "spider lightning" is a type of cloud-to-cloud lightning that occurs beneath stratiform clouds (low-level, thin clouds that may create a light drizzle) and flashes travel horizontally [16].



Figure 2.4: Intracloud [13].

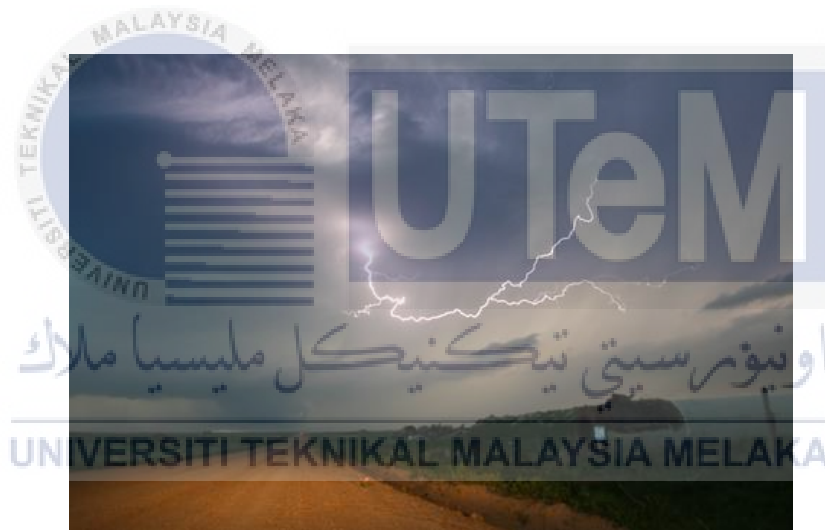


Figure 2.5: Cloud to air lightning [13].



Figure 2.6: Cloud to cloud lightning [13].

2.4 UNUSUAL FORMS OF LIGHTNING FLASHES

2.4.1 FORKED LIGHTNING

In some lightning strikes to the ground, the channel at the lowest point is split like a fork and seems to strike the ground at two different spots at the same time. Forked lightning is the name given to lightning flashes that have this characteristic. Forked lightning is caused by two physical conditions. The very first is as follows: The stepped leader produces multiple branches as it descends to the ground. As a result, many branches may be going toward the ground at any given time. The return stroke goes down the main channel as well as the branches, neutralizing the charges on the branches and halting their propagation. However, in extremely rare situations, another branch may contact the ground exactly after the main branch does, before its charge is neutralized by the main branch's return stroke [17].

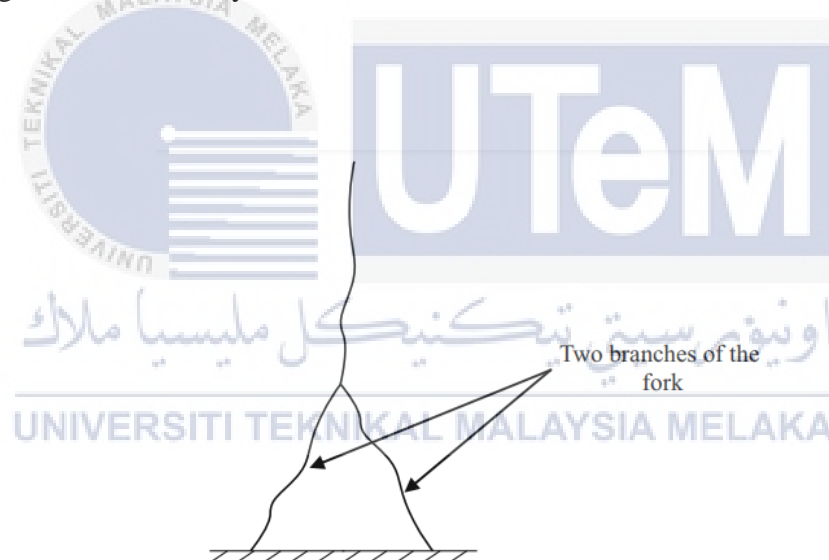


Figure 2.7: To the naked eye, forked lightning appears [17].

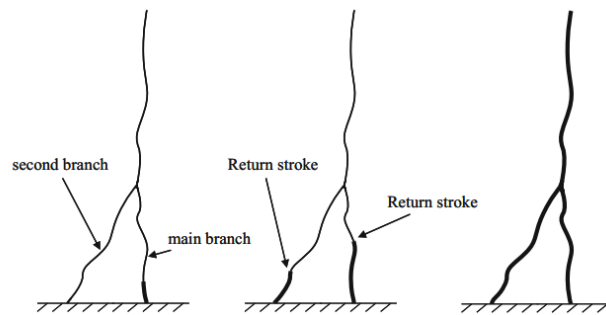


Figure 2.8: Process of return stroke for forked lightning [17].

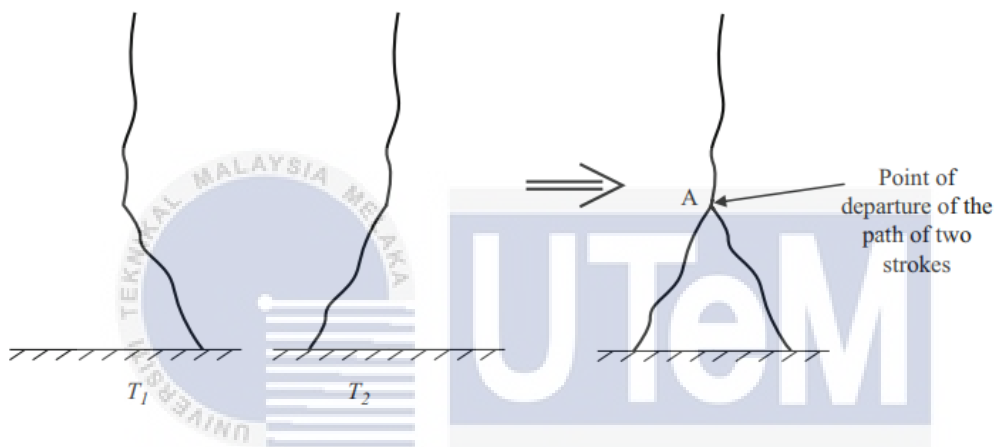


Figure 2.9: From a location below the thundercloud, two strokes of the same flash (separated in time by the amount $T_2 - T_1$) follow two different routes to ground (point marked A) [17].

UNIVERSITI TEKNIKAL MALAYSIA MELAKA

2.4.2 LIGHTNING WITHOUT THUNDER

When lightning flashes occur at a long distances, they are sometimes witnessed without any accompanying thunder. As a result of these lightning flashes, some people believe that some lightning flashes don't produce any thunder. In truth, all lightning flashes produce thunder as a result of the channel rapidly heating up during the return stroke. The diffraction of sound waves prevents the thunder from being heard. In heated air, sound waves travel quicker. Sound waves travelling in air are diffracted upward because the air layer near to the ground is warmer than the air at higher elevations, preventing them from reaching observers on the ground [17].

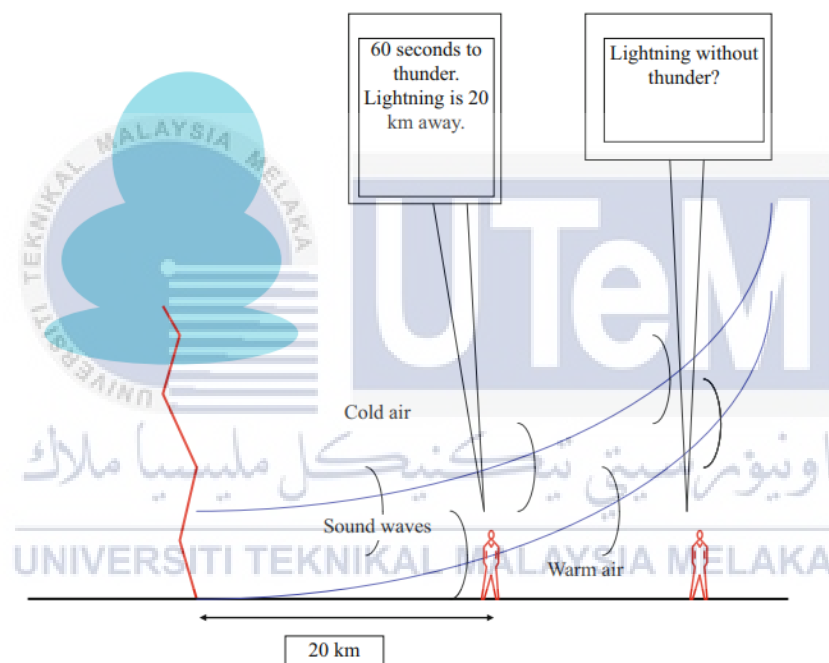
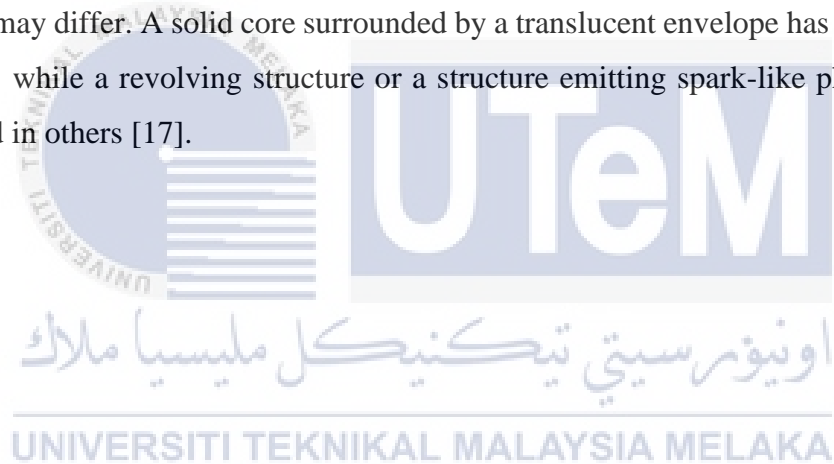


Figure 2.10: The occurrence of lightning without thunder [17].

2.4.3 BALL LIGHTNING

Because ball lightning cannot be created in a lab and the legitimacy of accessible images is in doubt, the features of ball lightning must be derived from eyewitness accounts. Ball lightning is described as spherical in shape by eyewitness accounts, while alternative shapes such as teardrops or ovals have also been observed. Ball lightning in the shape of rods has been seen on rare occasions. Ball lightning normally has a diameter of 10–40 cm, though it has been observed to have a diameter of 1 m. Ball lightning has a documented lifetime of about 10 seconds, however it has been recorded to linger up to 1 minute on rare occasions. Red, reddish yellow, yellow, white, green, and purple are some of the colors that might appear in ball lightning. Ball lightning's intensity may build over time, turning a brilliant white before disappearing explosively in some situations. From one report to the next, the structure of the ball lightning may differ. A solid core surrounded by a translucent envelope has been recorded in some cases, while a revolving structure or a structure emitting spark-like phenomena has been described in others [17].



2.5 MECHANISM OF LIGHTNING FLASHES

2.5.1 MECHANISM OF UPWARD INITIATE LIGHTNING FLASHES

Consider a tall building resembling a telecommunications tower. Consider the case if this tower is situated beneath a growing thundercloud. The electric field strength beneath the cloud increases as the charging process inside the cloud accelerates. It connects with the charge centers as it reaches the cloud, and a current akin to a continuous current begins to flow through this channel to ground. Dart leaders may travel down the channel and starting return strokes once the current stops. The absence of a stepped leader and the initial return stroke, as well as the presence of a sustained current at the start of the flash are the only differences between this and a typical lightning flash. The processes that occur during the dart leader–return stroke sequences are the same as those that occur during typical lightning flashes [17].

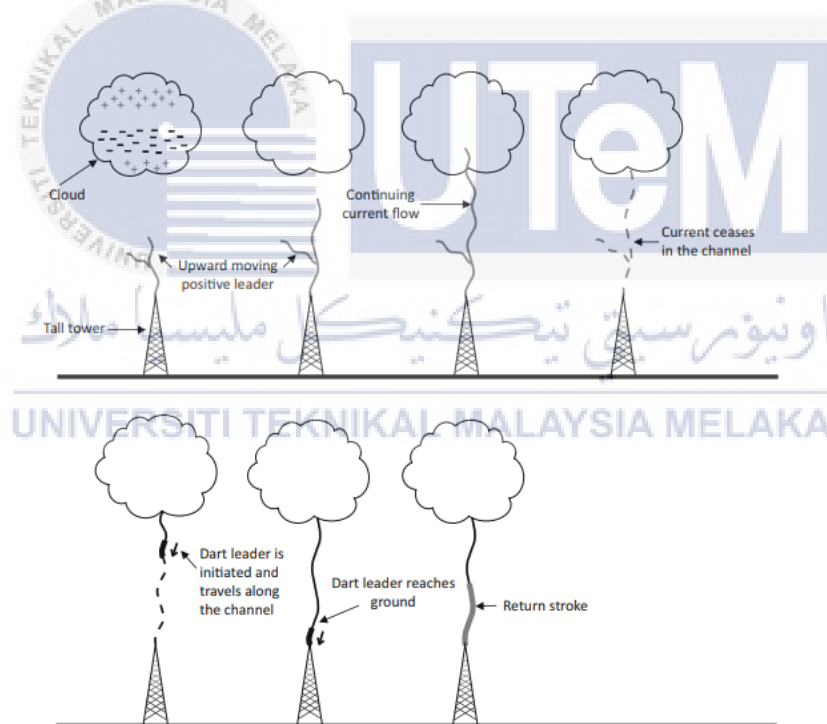


Figure 2.11: The basic characteristics of an upward initiated lightning flash [17].

2.5.2 MECHANISM OF POSITIVE GROUND FLASHES AND THEIR MAIN DIFFERENCE WITH NEGATIVE GROUND FLASHES

Positive ground flashes carry positive charges from the cloud to the ground. A positive flash usually comes from a location near the positive charge core. The leader is bidirectional, just like in a negative ground flash, but this time the negative leader end travels toward the positive charge center while the positive leader end travels toward ground. Positive ground flashes are usually caused by positive charge centers being shifted laterally from the negative charge center due to wind shear [24]. The positive leader travels more or less continuously toward ground, as is normal for leaders carrying a positive charge, but the channel brightness may alter from time to time throughout its propagation [17]. As a positive leader approaches the ground, it may generate a huge number of very faint branches, and bright recoil leaders occasionally move along these branches toward the main channel [18].



2.6 CLASSIFICATION OF LIGHTNINGS BY TYPES AND POLARITIES

There are two types of lightning flashes: those that strike the ground and those that do not. In many places around the world, the intracloud to cloud-to-ground lightning flash ratio has been researched extensively. Intracloud, intercloud, and cloud-to-air flashes (all of which do not involve ground) are estimated to account for 70–75 percent of lightning discharges, whereas cloud-to-ground flashes account for 25–30 percent. Negative CGs are the vast majority of cloud-to-ground flashes that transmit negative charge from the cloud to the ground. Positive CGs are ground flashes that transmit positive charge to the ground in around 10% of cases [19].

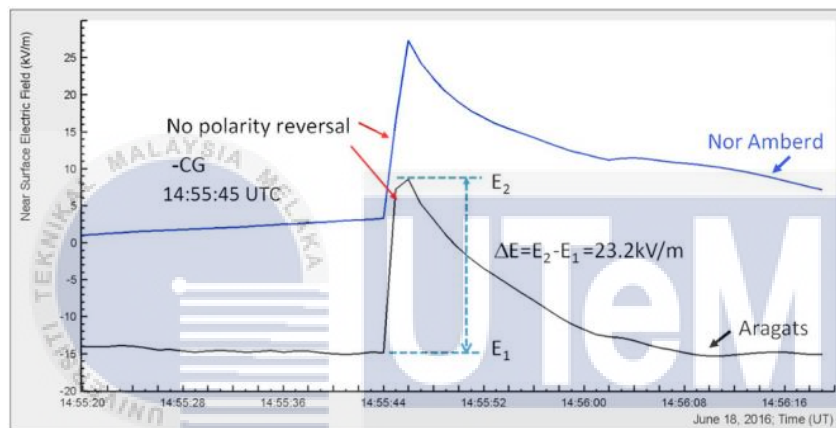


Figure 2.12: Electrostatic field changes produced by negative CG [19].

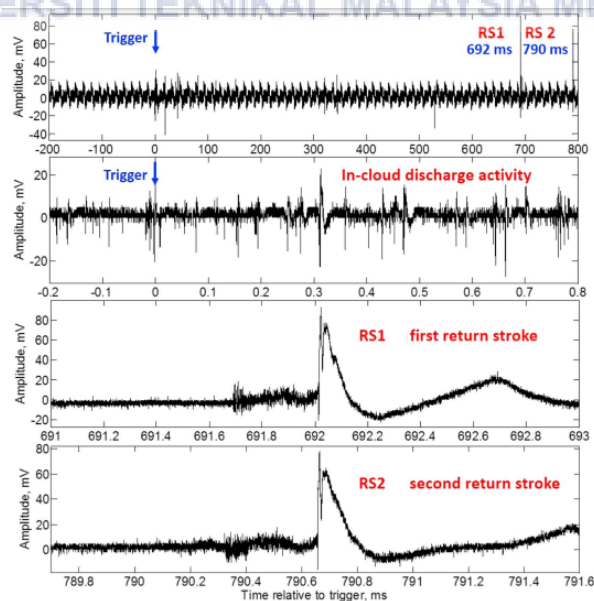


Figure 2.13: Fast electric field record of negative CG [19].

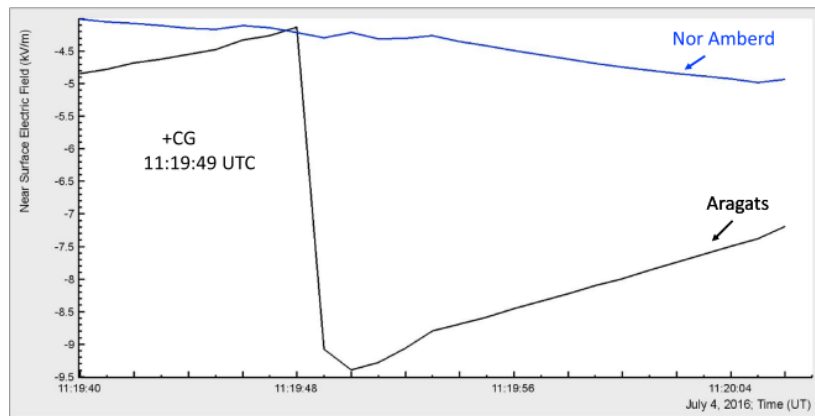


Figure 2.14: Electrostatic field changes produced by positive CG [19].

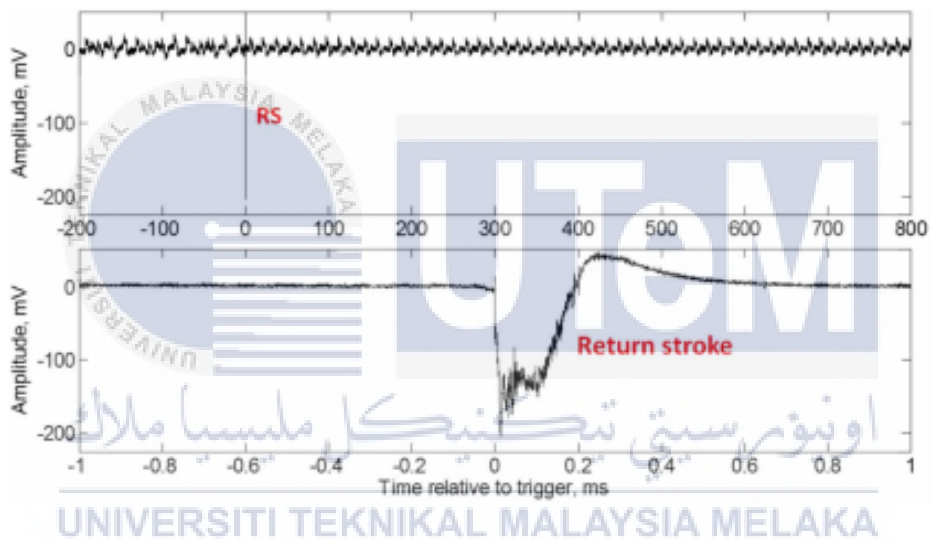


Figure 2.15: Fast electric field record of positive CG [19].

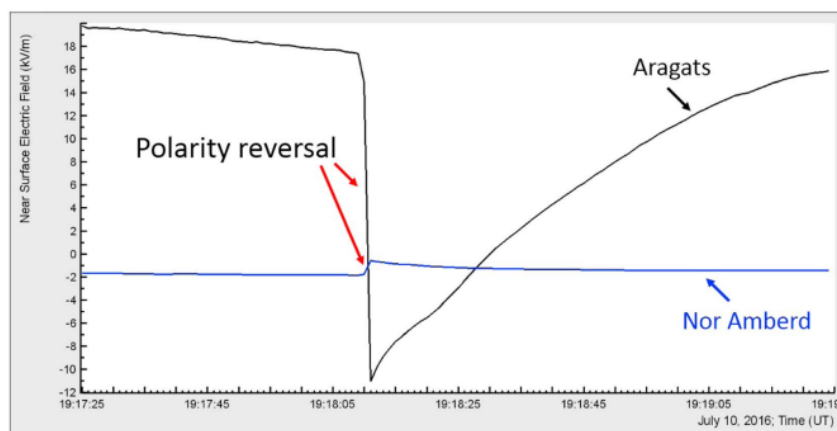


Figure 2.16: Electrostatic field changes of opposite polarity produced by inverted-polarity IC flash [19].

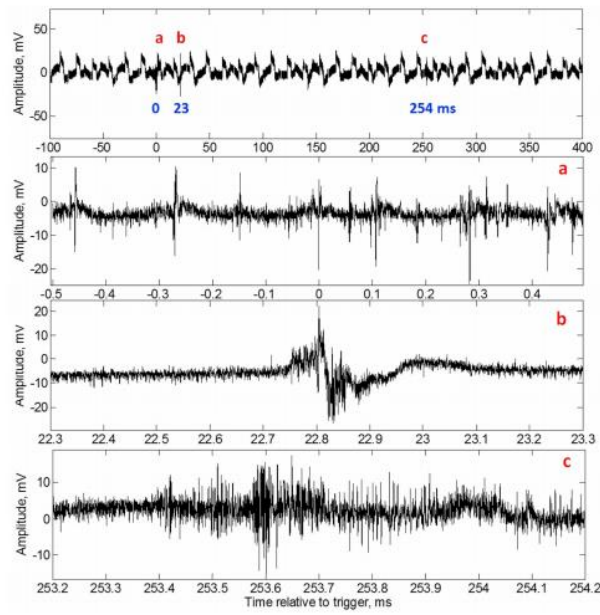


Figure 2.17: Fast electric field record of inverted-polarity IC flash [19].

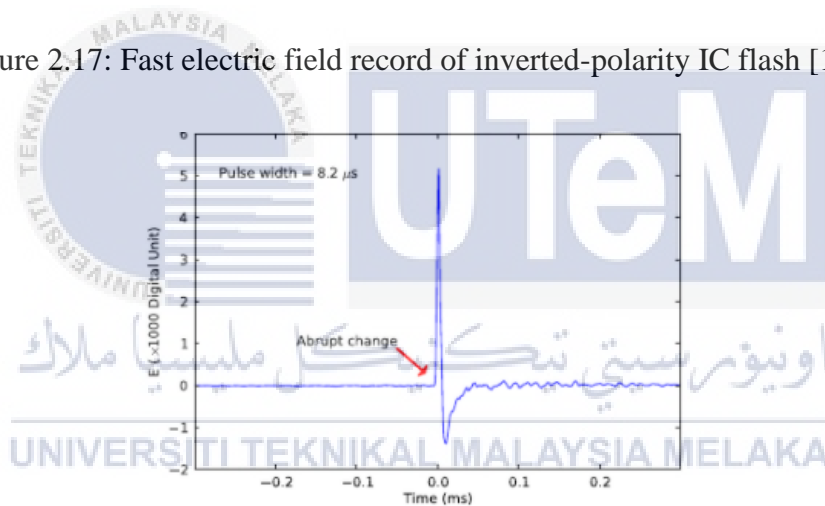


Figure 2.18: Negative NBE [20].

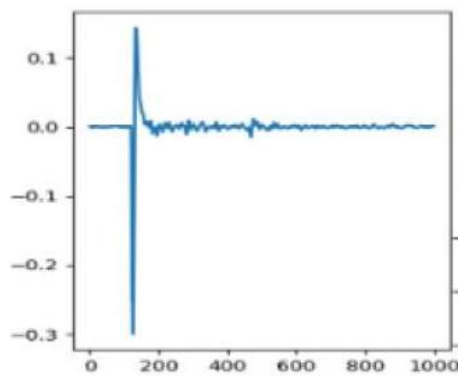


Figure 2.19: Positive NBE [21].

2.7 LIGHTNING STRIKE

Lightning flashes can be divided into two types which those strike the ground and do not strike the ground. These two groups are further split according to the route and direction of the current in the bright channels associated with each flash [22]. Lightning strikes are a significant cause of transient over voltages, which can cause in defects. A nearby strike can elevate the local ground potential, resulting in neutral current flowing to earth via a remote ground, which can be damaging to sensitive equipment [23]. Although a lightning strike is an unusual type of trauma, it is one of the primary causes of cardiac arrest and death due to natural disasters [24,25].

Moreover, there are some characteristics of lightning strikes which include polarity, highest peak current, and number of return strokes change with time and space. Geography, topography, and large-scale weather patterns all affect these differences [26]. Return strokes which consist of current surges that last only a few microseconds during lightning strikes. Return strokes for negative strikes can range from one to numerous, whereas positive strikes normally only have one [26]. Uman (1987) reported that majority of lightning strikes are negative which is 90%, only 10% is positive; therefore, the average of number of strokes is 3-4 per negative strike and 1 per positive strike; negative strikes have long continuing current in 20%-40% of cases, whereas positive strikes have them in 50%-100% of cases [27].

2.8 LIGHTNING DISCHARGE

2.8.1 PRELIMINARY BREAKDOWN PULSE

Ground flash is a word used to describe a negative cloud-to-ground lightning discharge that consists of three to five component strokes or merely strokes [28]. The development of a single channel or a sequence of channels is the first step in the breakdown process [29]. The lower border of a negative charge core is usually where a negative ground lightning flash begins. The breakdown process is accelerated by the improvement of electric field that generated by a positive charge pocket placed below the negative charge core, known as preliminary breakdown pulses (PBP) or first breakdown pulses [30].

The initial polarity of the PBPs has always been negative for negative return strokes [31]. The return strokes are frequently preceded by three discharge processes known as the initial breakdown (also known as preliminary breakdown (B), intermediate (I), and stepped leader (L) [32]. A stepped leader (L) is frequently used after the preliminary breakdown (B) stage, either directly or after an intermediate (I) stage [33]. Positive lightning's return stroke is occasionally preceded by a train of bipolar pulses (or PBP) lasting a few milliseconds [34].

The greatest amplitude of PBP is normally much smaller than that of the following return stroke, however it can occasionally be comparable to or even larger [35]. In negative cloud-to-ground (-CG) lightning, the initial polarity of PBP is always the same as the first return stroke [9]. The situation with positive cloud-to-ground (+CG) lightning, on the other hand, is far more complex [9].

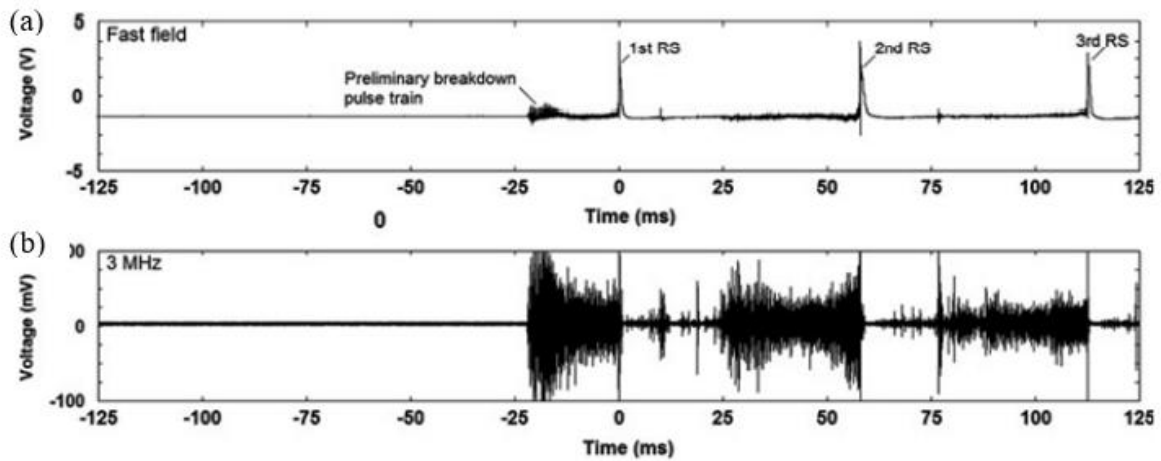


Figure 2.20 (a): 3 return strokes of lightning flash that captured by FA system at 10-20km [17].

Figure 2.20 (b): high-frequency (HF) radiation at 3 MHz [17].

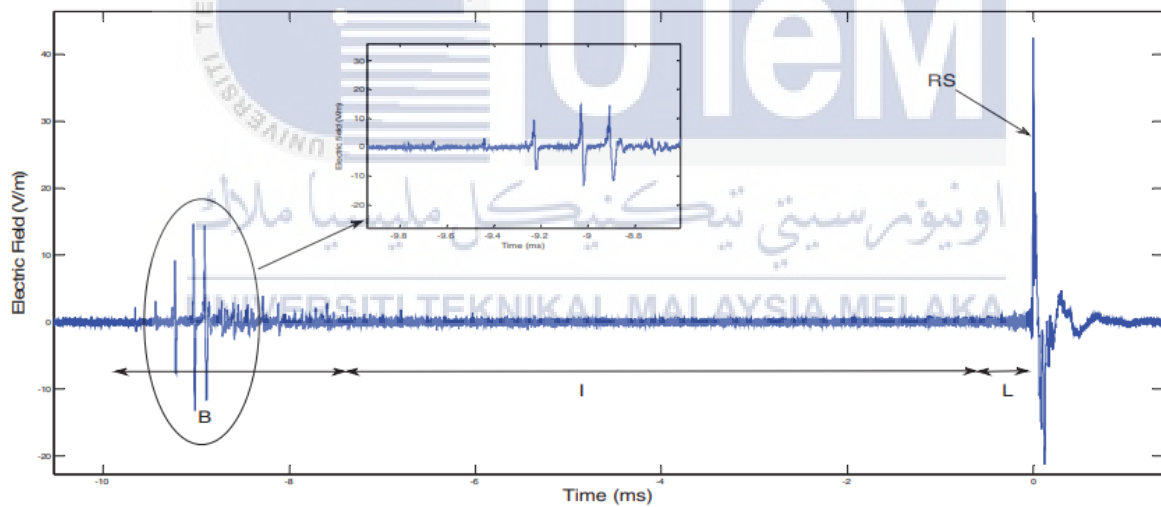


Figure 2.21: A clear preliminary breakdown pulse train, intermediate, and tiered ladder can be seen in this example of negative cloud-to-ground lightning [33].

2.8.2 STEPPED LEADER

Stepped leaders develop within thunderstorm clouds when charge differences between the main region of negative charge in the middle of the thunderstorm and the small region of positive charge near the base of the storm become large. When charge differences in the cloud get even more high, stepped leaders emerge. When this happens, the air's insulating capability degrades, and the negative charge begins to go downstream [36]. It moves in step toward ground, as is typical of the negative end of a bidirectional leader. A stepped leader is a negative leader that travels toward the ground in a stepped manner [17].

Besides that, the stepped leader seems to propagate toward the ground in intermittent steps in a photographic record. Each step is around 10–100 m long, with a time interval of around 10–100 s between them. The leader conveys a negative charge from the cloud to the ground, and this charge is stored both in the core and in a zone around the core known as the corona sheath in any particular channel section [37].

The leader's path from cloud to earth can be quite erratic and indirect. Therefore, as it goes aimlessly toward the ground, the leader does not pick the path of least resistance from cloud to ground [37]. In addition, as it seeks a link to the ground, the stepped leader usually branches outward. Experiments have shown that step formation can occur at speeds of up to 108 m/s [38]. As there is a delay between steps, the stepped leader's average downward speed is around 3×10^5 m/s [39].

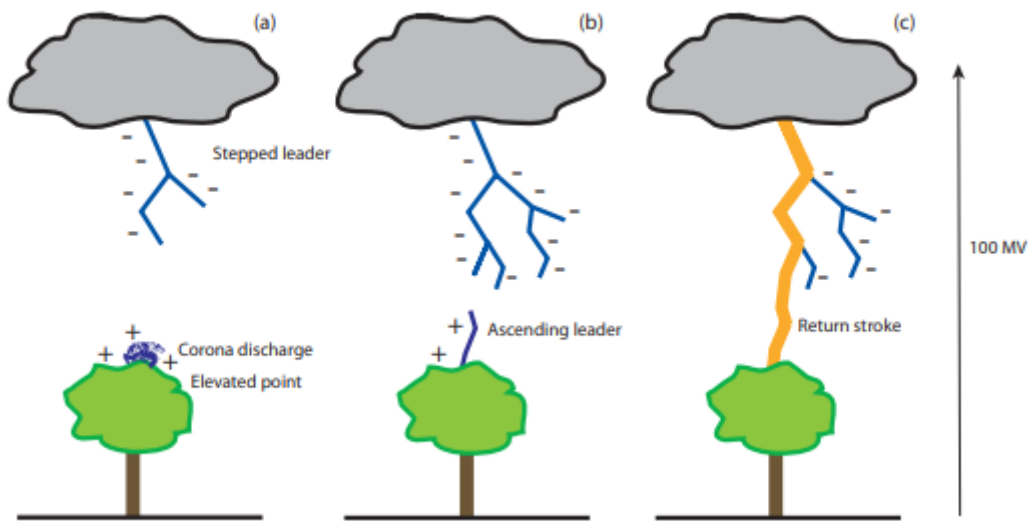


Figure 2.22: Mechanism of lightning initiation: (a) stepped leader formation; (b) initiation of an upward leader; (c) return stroke [40].

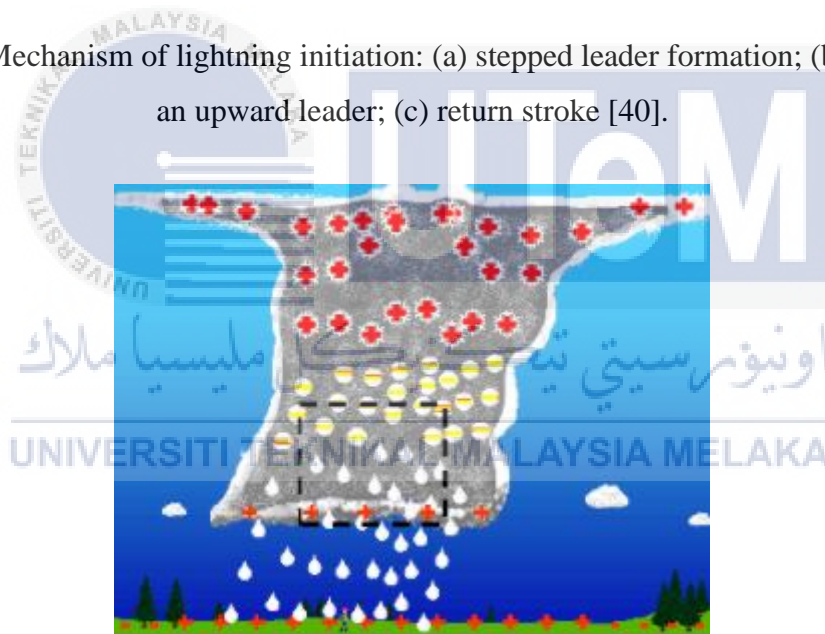


Figure 2.23: Charge of stepped leaders [37].

CHAPTER 3

METHODOLOGY

3.1 INTRODUCTION

This chapter describes an overview of the instruments and software used for the data collection in this research such as electric field mill (EFM), fast electric field antenna system (FA), weather radar and world wide lightning location network (WWLLN). It provides the information and method to analyze the lightning data, radar data and WWLLN data.

3.2 DATA COLLECTION AND TOOL

There are four types of data will involve in this research such as electric field change, lightning data, radar data and WWLLN data. The lightning data are collected from electric field mill (EFM), fast electromagnetic field antenna system (FA), and world wide lightning location network (WWLLN). While the radar data are obtained from Malaysia Meteorological Department (MMD). The duration of lightning data and radar data collected is 10 hours which started from 4am until 2pm on 11 August 2020. The location to collect the data is at Malacca.

3.2.1 ELECTRIC FIELD MILL (EFM)

At Universiti Teknikal Malaysia Melaka (UTeM), the EFM sensor has been installed. When lightning is detected, the EFM-100 Electric Field Mill short-range sensor (20 miles/32 km) regularly detects for lightning and activates graphical display alerts on a computer or laptop. There are two high electric field alarms, as well as lightning distance ranges that can be customized to notify you when nearby lightning. When no lightning is detected during the defined time period and the electric field levels fall below the defined levels, the programme will reset to a green All Clear status [41].

The static atmospheric electric field at the instrument's location is measured by EFM. They work by exposing a sensor element to the electric field and an uncharged reference in alternating sequences. The external electric field charges the sensor element, which is then discharged when exposed to the uncharged reference. Charge amplifiers transform the induced charge of the sensor element to a voltage that is proportionate to the external electric field [42].

EFMs have a restricted range in terms of the area for which the resulting lightning warnings are valid as they measure the local atmospheric electric field. This range is also affected by factors such as orography, surface type, surrounding buildings, vegetation, and so on [42].

Even without a thunderstorm nearby, the local electric field changes from location to location. As a result, the strength of the local electric field over which a warning is sent varies from location to location. As a result, each location's trigger level must be set separately [42].

EFMs detect a range of different signals not related with thunderstorms in addition to the effects of charge separation in thunderclouds. Blowing sand or dust, blowing snow, charge separation in non-lightning showers, and charge separation when raindrops splash on or near the instrument are examples of these [43].

During a thunderstorm, EFMs detect relatively gradual field changes (on the order of tens of seconds to minutes) caused by charge separation processes in the cloud, as well as the evolution and final dissipation of net charge regions as the storm progresses. Moreover, they also detect quicker (time scale 1 sec) changes caused by lightning rearranging cloud charge. Field changes produced by lightning can cause the field to grow above or fall below a threshold utilized in a warning algorithm [43].



Figure 3.1: Electric field mill (EFM) sensor [41].

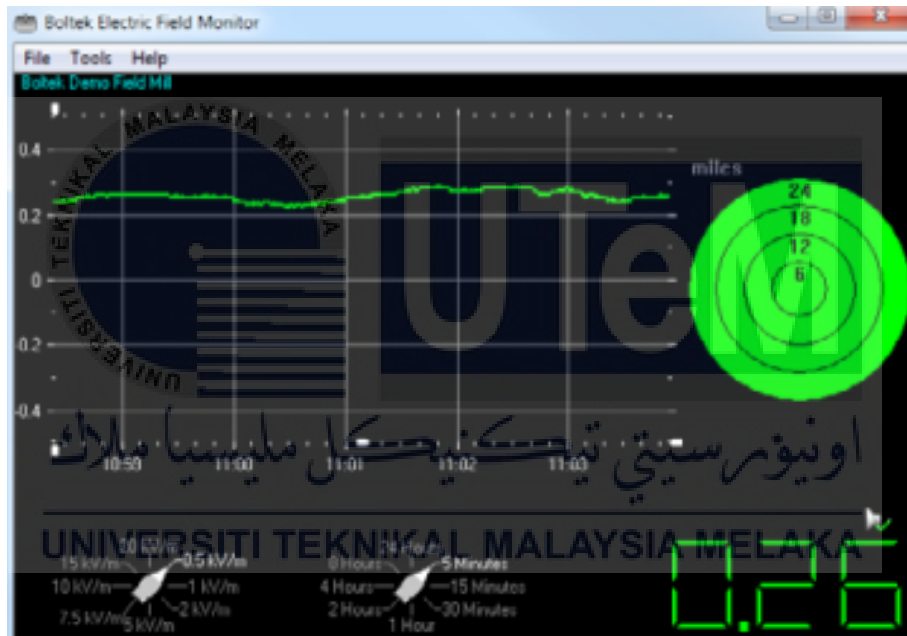


Figure 3.2: Electric field monitor software shows all clear status [41].

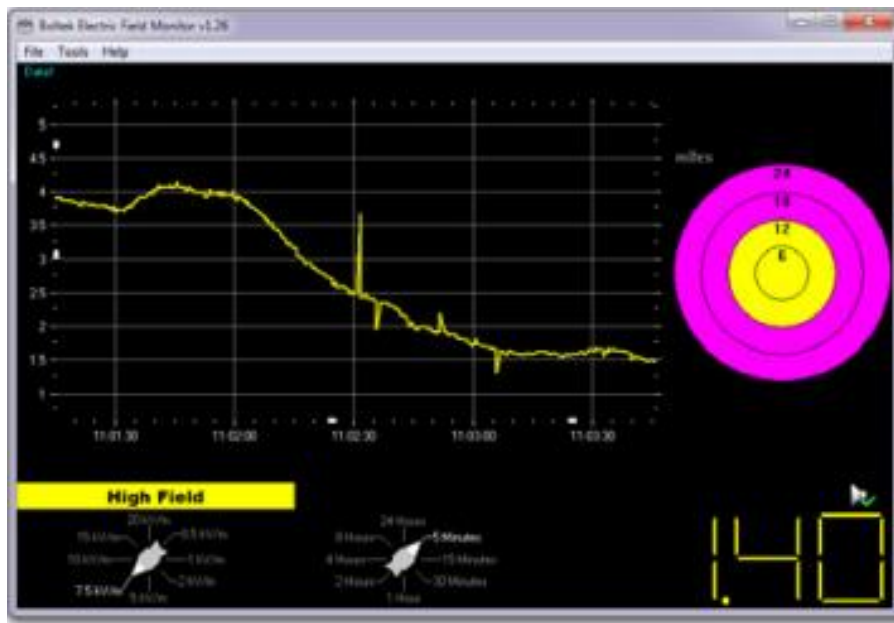


Figure 3.3: Electric field monitor software shows lightning and high field alarm active

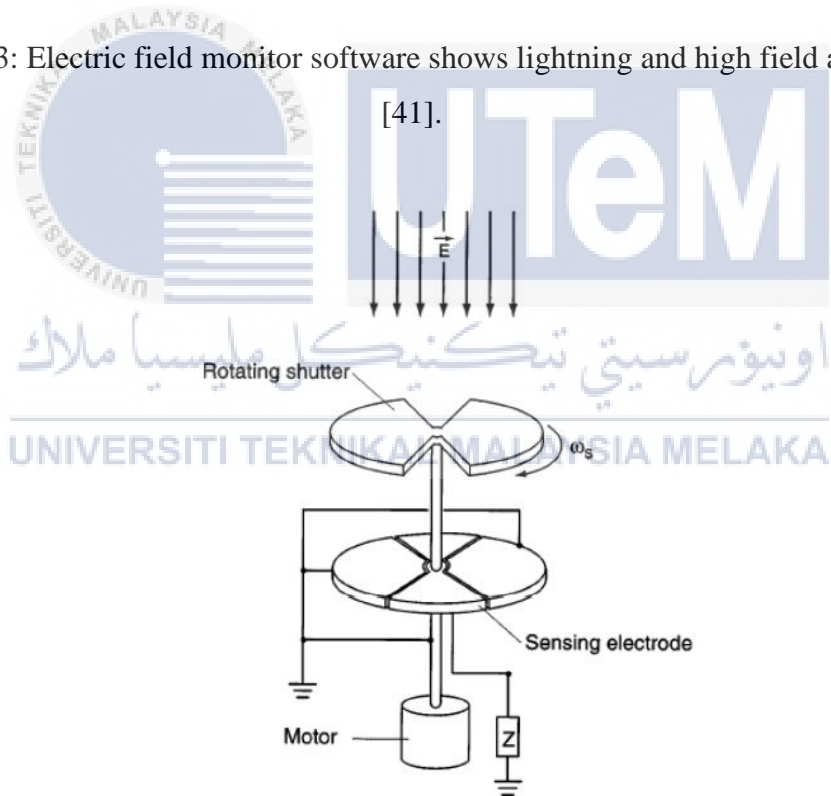


Figure 3.4: Schematic of a shutter-type EFM [42].

3.2.2 FAST ELECTROMAGNETIC FIELD ANTENNA SYSTEM (FA)

Cooray and Lundquist (1982) described quick and slow electric field measuring antenna devices that were identical. The antenna was connected to the electronic buffer circuit with a 60 cm length coaxial cable (RG58). The transient recorder was set to a pre-trigger mode of 300 milliseconds. For the step input pulses, the rising time of the broadband antenna system (fast field) was less than 30 ns, and the fading time constant was set to around 15 ms. The slow antenna system's decay time was set to 1 second. The HF antenna system's resonance frequencies were determined to be 3 and 30 MHz, with 3 dB bandwidths of 264 kHz and 2 MHz respectively [44].

VHF emission from IC flashes was observed using a single observation (OS) system with fast and slow electric field antenna systems with decay time constants of 13 ms and 1s respectively, and a VHF sensor (bandwidth 40-80 MHz) with a 60 MHz center frequency. The OS is located at Universiti Teknikal Malaysia Melaka (UTEM), Malacca, Malaysia (2.314077° N, 102.318282° E). The coaxial wire for the fast and slow electric field antenna systems was fixed at 10 meters, and the VHF sensor was connected to the oscilloscope via a 5 meter cable [45].

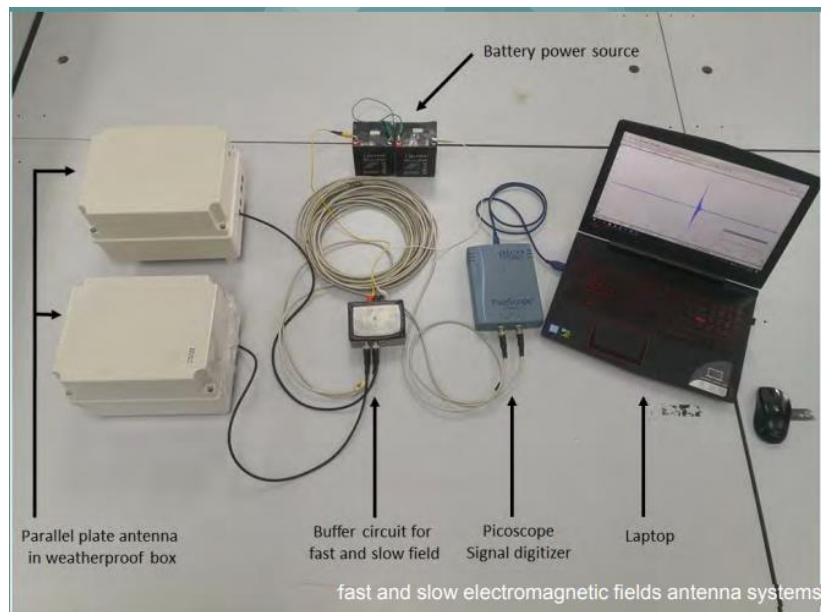


Figure 3.5: Setup of fast and slow electromagnetic fields antenna system [46].



Figure 3.6: Fast and slow electromagnetic field antenna system that located at Universiti Teknikal Malaysia Melaka (UTEM), Malacca, Malaysia (2.314077° N, 102.318282° E) [46].

3.2.3 WHEATER RADAR

The reflectivity product for local radar bases is a diagram of echo intensity (reflectivity) in decibels (dBz, decibels). When compared to the reference power density at 1m from the radar antenna, reflectivity is the amount of transmitted power returned to the radar receiver after striking precipitation [47]. The Universiti Teknikal Malaysia Melaka hosts a single measurement station (OS) with a wideband electric field antenna system (decay time constant 13 ms), a narrowband electric field antenna system tuned to 3 MHz (HF), and a pair of orthogonal wideband magnetic field antennas. The Malaysia Meteorological Department (MMD) provided radar data in the Constant Altitude Plan Position Indicator (CAPPI) format. The CAPPI was chosen because of its ability to display high-resolution images that can be easily studied.

One of the most significant recent developments in hydrologic engineering and practice is radar-derived rainfall estimation. In hydrologic modelling, there is a trade-off between rainfall data gathered by rain gauges and rainfall data obtained by radar. Rain gauges offer point data for rainfall depth and intensity, but they are inefficient at supplying information on rainfall distribution. While rain gauges may be adequate for widespread rain events, a gauge network may completely miss small convective rainfall events. Rainfall data collected from radar provides a density of measurements not available with rain gauges alone. When these two sensor systems are combined, better rainfall estimations are obtained, which better define rainfall over a watershed [48].

A radar does not directly detect rainfall totals; instead, it uses an empirical relationship with the radar reflectivity factor, Z (mm^6/m^3) to estimate rainfall rate, R (mm/h). Rainfall rates are proportional to the volume of raindrops, yet reflectivity is related to the drop diameter divided by the sixth power [49]. To convert from reflectivity to rainfall rate, a raindrop size distribution must be considered. The Z-R relationship converts reflectivity into a rainfall rate using the formula:

$$Z=aR^b \quad (1)$$

where a and b are constants. Because of changes in raindrop size distribution, the Z-R relationship values change as a function of precipitation types, which is a significant issue [50].

Z stands for reflectivity and is measured in mm^6/m^3 . Reflectivity can range from one to six orders of magnitude. As a result, expressing Z in decibels ($\text{dBZ} = 10\log_{10}$) is frequently more convenient [51].

Radar can be used to estimate how hard it is raining. Light rain is defined as reflectivity values below approximately 35 dBZ; moderate rain is defined as reflectivity values between 35 and 50 dBZ; and heavy rain is defined as reflectivity values above about 50 dBZ. Hail is commonly defined as a reflectivity value of more than 55 dBZ [52].

Different colors are used to determine the intensity of the falling rain or snow. While color palettes for precipitation might vary, the colors listed below are the most frequent. Based on the Figure 3.8,

- Light green= Light rain or rain [53]
- Dark green= Light to moderate rain [53]
- Yellow= Moderate rain [53]
- Orange= Heavy Rain [53]
- Red= Very Heavy Rain or Rain & Hail [53]
- Purple= Extremely heavy rain or hail [53]

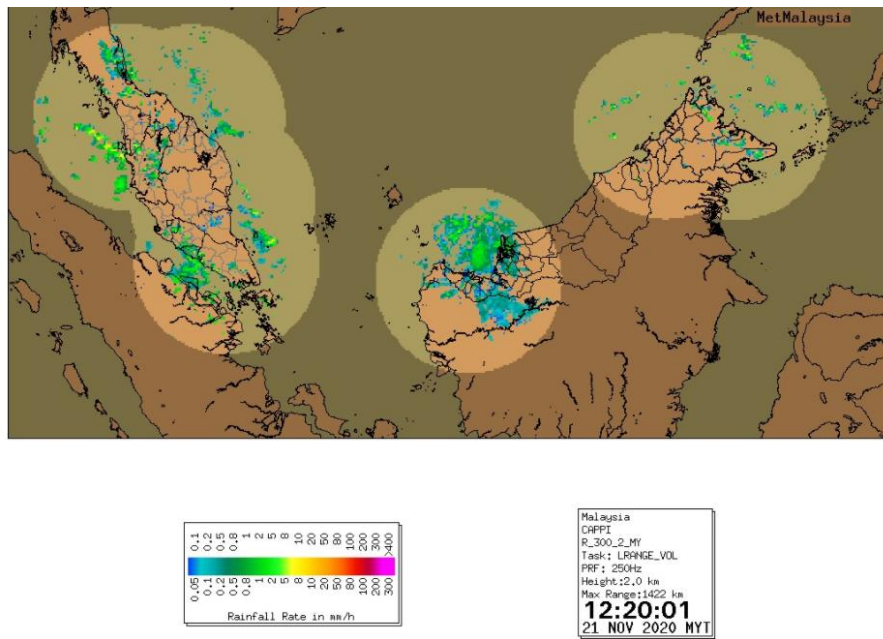


Figure 3.7: Radar Malaysia map [54].

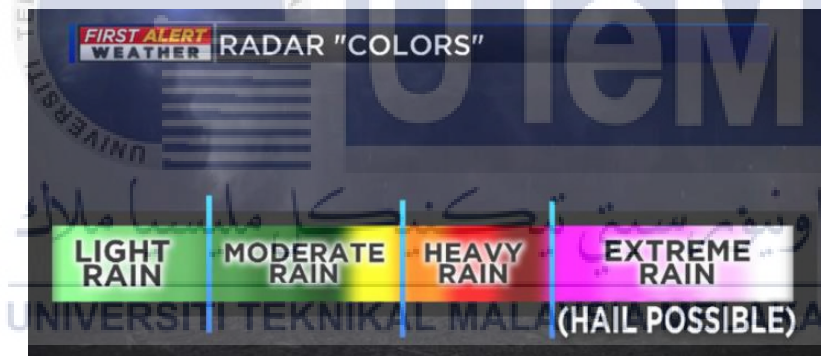


Figure 3.8: The meanings of radar color [53].

Table 3.1: The Z-R relationships [55].

| Relationship | Optimum for | Also recommended for |
|---|----------------------------------|-------------------------------|
| Marshall-Palmer (MP)($Z=200R^{1.6}$) | General Stratiform precipitation | Other non-tropical convection |
| Convective (WSR-88D)($Z=300R^{1.4}$) | Summer deep convection | |
| Rosenfeld Tropical (RT)($Z=250R^{1.4}$) | Tropical convective systems | |

3.2.4 WORLD WIDE LIGHTNING LOCATION NETWORK (WWLLN)

The World Wide Lightning Location Network was created to fulfill the requirement for a global and real-time lightning detection system. Where regional networks are unavailable, this network can offer high-quality lightning data over maritime and remote region. The network also provides continuous detection throughout time, which satellite equipment do not do [56].

Lightning discharges emit very low frequency (VLF; 3-30 kHz) radiation, which is measured by the network stations. Propagation at these extremely long electromagnetic wavelengths (up to 100 km) allows lightning strokes to be tracked in real time up to 10,000 kilometers away from the receivers, with a position precision of a few kilometers. The use of frequencies below roughly 30 kHz is required for true global mapping of lightning from widely dispersed (a few Mm) ground-based receivers. Lightning impulses in this frequency range have low propagation attenuation, therefore they can travel long distances in the Earth-ionosphere waveguide [57,58].

Instead of using the spheric Time of Group Arrival (TOGA), the WWLLN operated in a simple mode during its initial testing phase, delivering station trigger times to a central processing point. As expected, the introduction of the TOGA algorithm considerably enhanced location accuracies. The global location accuracy ranges from 2 to 20 kilometers, with a global median of 3 kilometers and a global mean of 3.5 kilometers [Rodger et al. 2005]. WWLLN detection effectiveness is dependent on peak current, according to regional case studies, with high peak current strokes having a higher detection efficiency than low peak current strokes [Lay et al. 2004; Rodger et al. 2004].

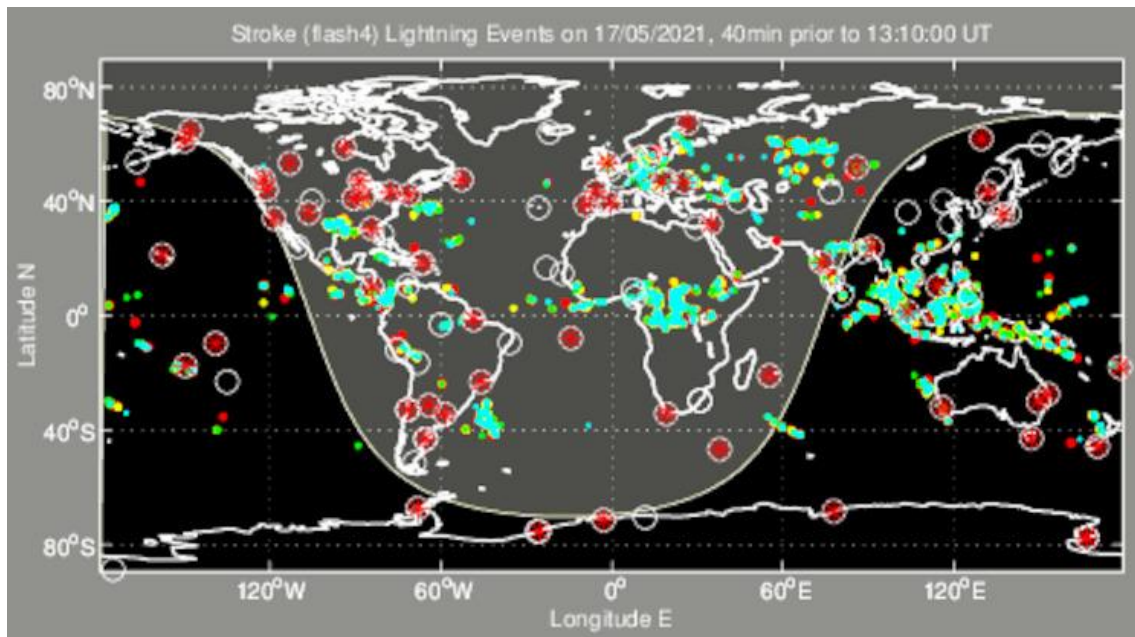
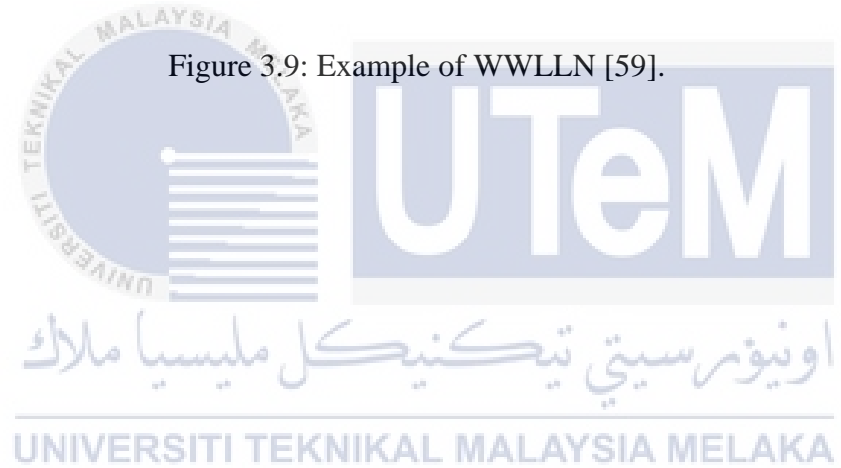


Figure 3.9: Example of WWLLN [59].



3.3 DATA PROCESSING

In this study, we used the lightning data that collected from the EFM, FA system, weather radar and WWLLN in Malacca for the purpose of analysis. The duration to collect the data is 10 hours which started from 4am until 2pm on 11 August 2020. The observation area is set at Malacca, Malaysia. Figure 3.10 showed the flowchart of this research.

Firstly, before processing again with MATLAB software, the EFM data required to be filtered first using code in the MATLAB programme to guarantee data quality and guarantee there were no missing data. The MATLAB software made it simple to analyze the lightning data and determine when the electric field changed the most.

Furthermore, the lightning data that collected by using FA system and the data are saved in PSDATA file. Picoscope 6 software is used to open the PSDATA file and then analyze the types of lightning flashes based on the waveform that detected by FA system. Picoscope 6 is primarily used to observe and analyze real-time signals captured by Picoscope oscilloscopes and data loggers. The software allocates as much display space as possible to the waveform or waveforms. This ensures that the waveform has the best possible view and that the largest quantity of data is displayed [60]. Besides that, Figure 3.11 showed the representation of each color lines such as blue color line represented fast electromagnetic field antenna, red color line represented slow electromagnetic field antenna, green color line represented polarity of North and South, and brown color line represented polarity of East and West. Figure 3.12, 3.13 and 3.14 showed the example waveform that captured by FA on 11 August 2020. Based on these waveforms, type and characteristics of lightning flashes are observed. Then the results obtained are put into the Microsoft Excel. Based on the results obtained by FA system, flash rate on 11 August 2020 can be determined also.

In addition, the radar data are obtained from Malaysia Meteorological Department (MMD) and the files are in CAPPI format. Based on Figure 3.15, rainfall rate can be examined by using the color gauge. However, there is a relationship between rainfall rate and reflectivity. The value of reflectivity can be determined based on this relationship. Based on the radar data, the movement of rainfall also can be examined.

Moreover, The WWLLN is a global lightning detection network that was created through international collaboration, is sponsored by scholars all over the world who host sensors and is coordinated at the University of Washington [61]. For WWLLN AE data, stroke count data is provided as ASCII text format files. The AE data contains the date and timestamp to the nearest microsecond, latitude and longitude in decimal degrees, and lightning strike energy (J). Figure 3.16 showed the coding to obtain the AE data in Excel file. The area of observation is at Malacca, Malaysia (latitude: $2^{\circ}11'45.6''$ N, longitude: $102^{\circ}14'25.8''$ E). Therefore, line 11 and line 12 that showed in Figure 3.16 represented the range of latitude and longitude of whole area of Malacca. Then, time in AE data that in Universal Time Coordinated (UTC) is converted to Malaysian Standard Time (MYT). Number of lightning strikes, coordinate that lightning strike occurred and energy of lightning strike are analyzed. After that, the location of lightning strike is observed by using Google Earth Pro.

Lastly, electric field, lightning flashes, rainfall rate and WWLLN data are correlated.

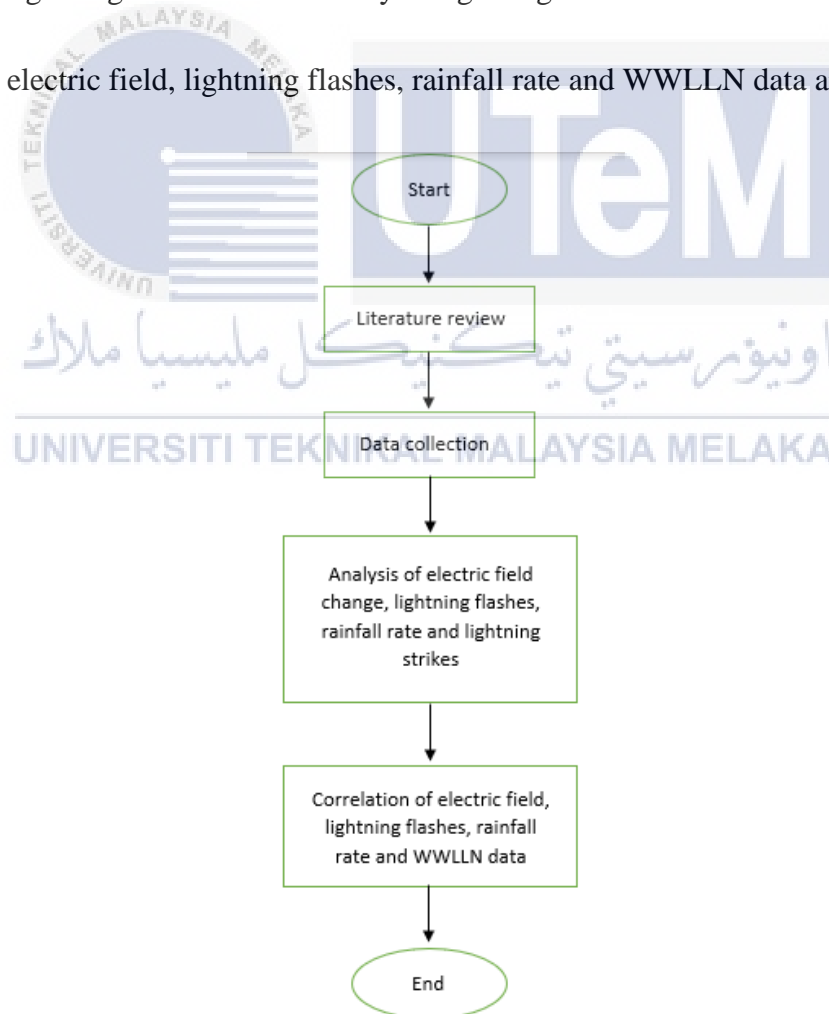


Figure 3.10: Flow chart of the research.

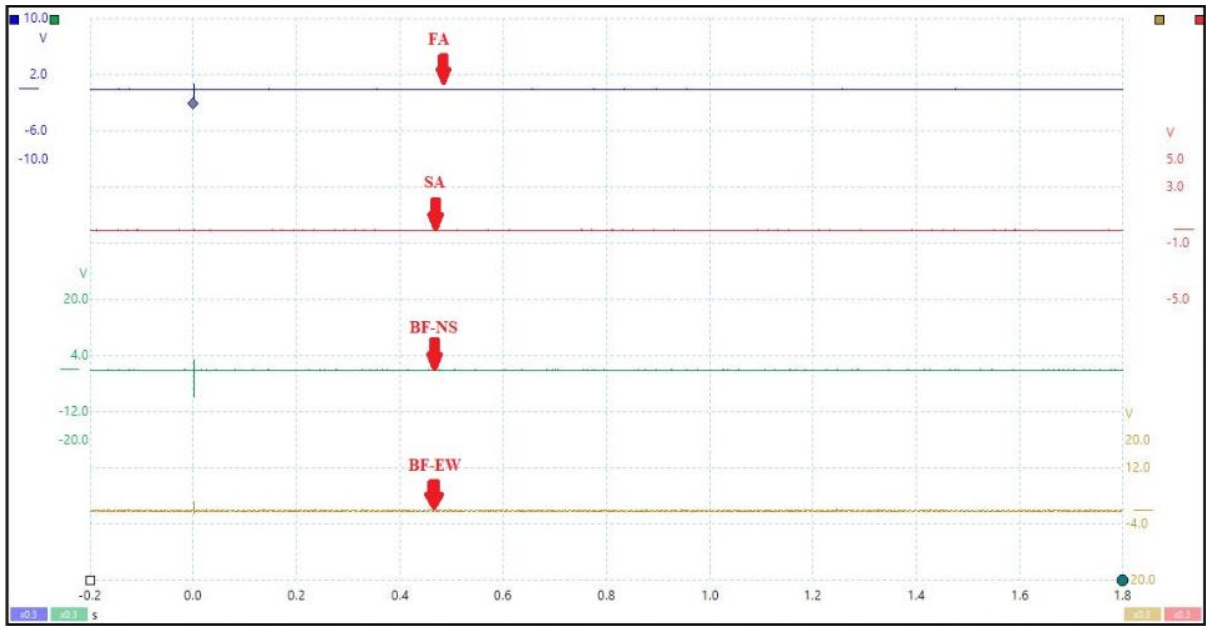


Figure 3.11: Representation of each color lines in Picoscope 6 software.

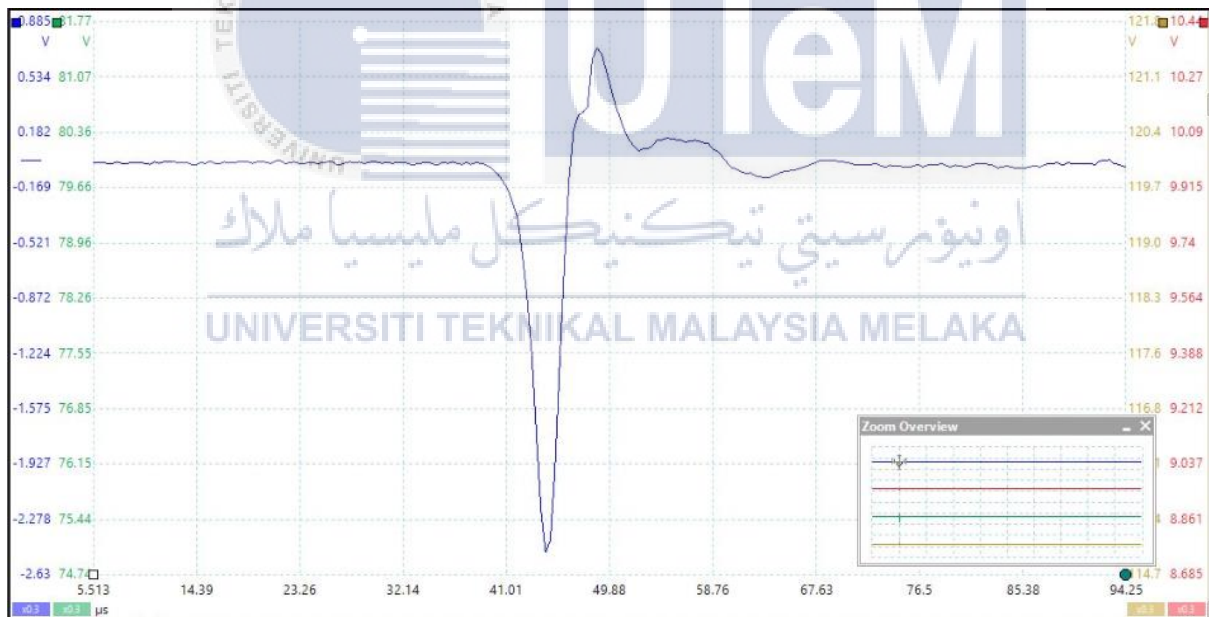


Figure 3.12: Example waveform that captured by FA system at 04:02:18 on 11 August 2020 in Malacca.

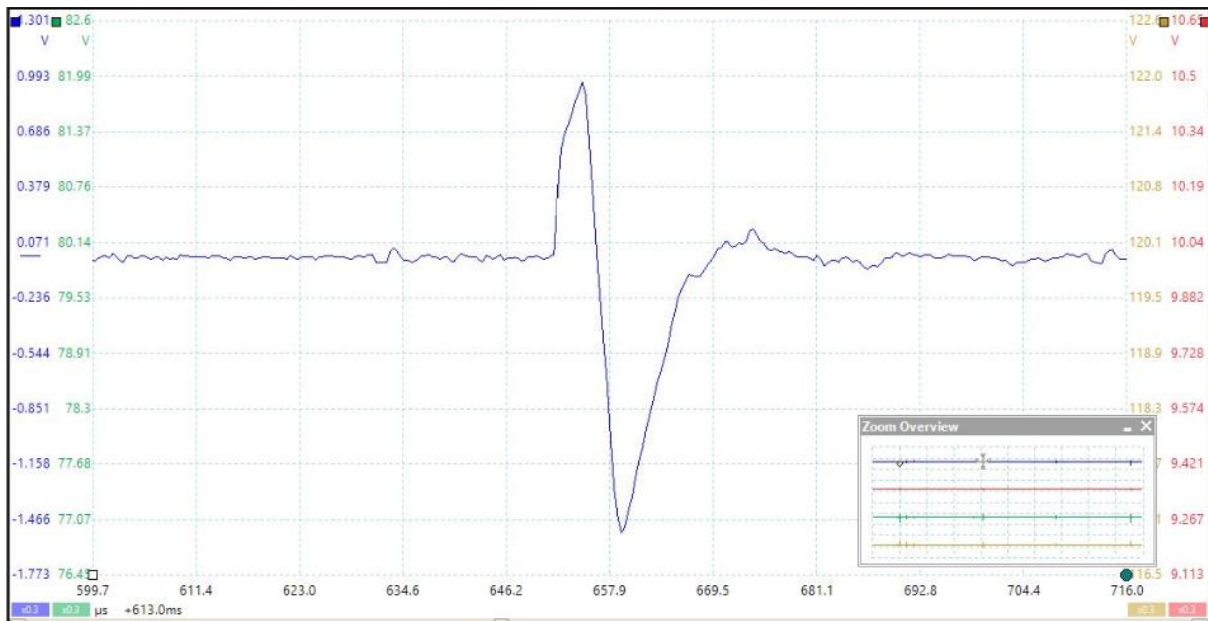


Figure 3.13: Example waveform that captured by FA system at 05:46:40 on 11 August 2020 in Malacca.

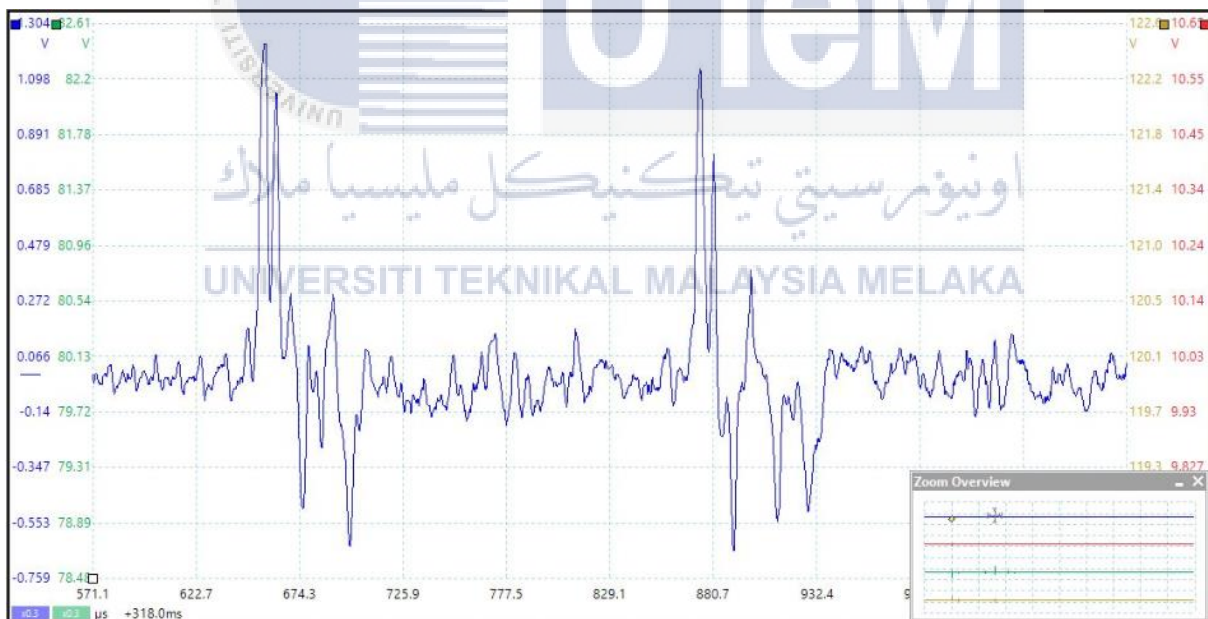


Figure 3.14: Example waveform that captured by FA system at 05:47:28 on 11 August 2020 in Malacca.

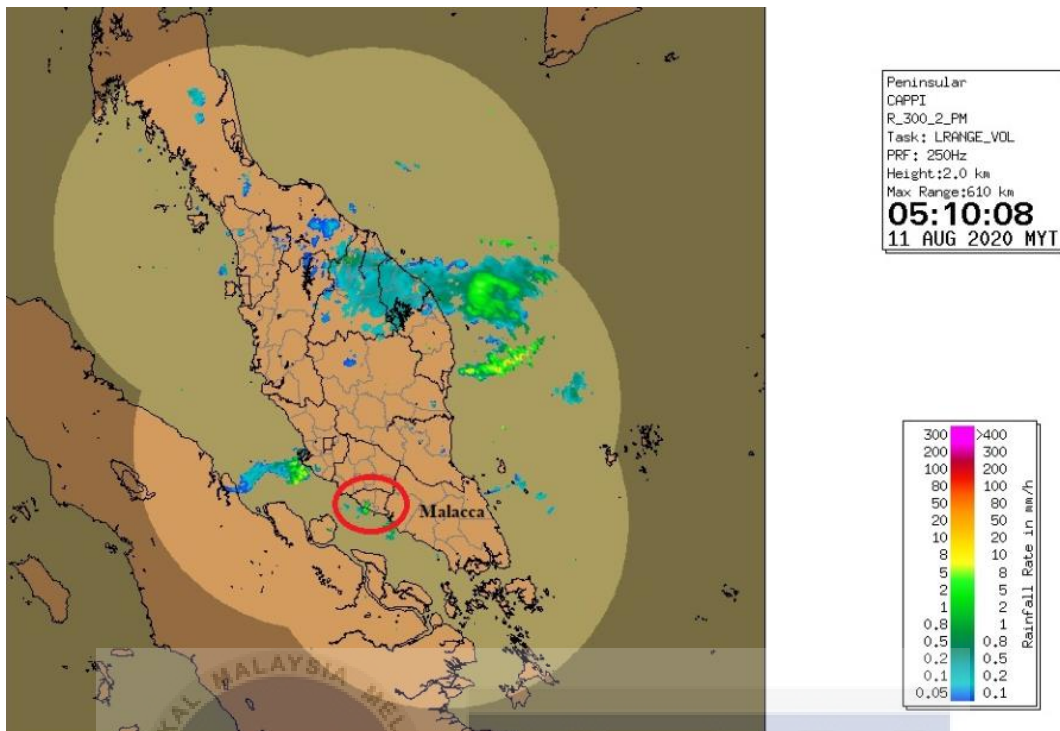


Figure 3.15: Example of radar data at 05:10:08 on 11 August 2020.

```

Editor - C:\Users\Asus\Desktop\ww\ln\Untitled8.m
Untitled8.m  x +
1 - for count=1:31 %if error put 31:1
2 -   file_names = sprintf('AE202008%02',count); %change based on year and month eg: AE202008%02
3 -   load (file_names);
4 -   col_header={'Latitude','Longitude','Hour','Min','Second','Energy'};
5 -   %operations
6 -   N = length(data);
7 -   j=1;
8 -
9 -   newdata=[];
10 -   for i=1:N
11 -     if data(i,7)>=2 && data(i,7)<=2.5 %latitude margin change according to area of observation
12 -       if data(i,8)>101.9 && data(i,8)<=102.6 %longitude margin change according to area of observation
13 -         newdata(j,:) = [data(i,7) data(i,8) data(i,4) data(i,5) data(i,6) data(i,11)];
14 -         j=j+1;
15 -       end
16 -     end
17 -     i=i+1;
18 -   end
19 -
20 -   if isempty(newdata)==0
21 -     save_files = sprintf('AE202008%02',count); %change similar as year month above
22 -     xlswrite(save_files,col_header,'Sheet1','A1');
23 -     xlswrite(save_files,newdata,'Sheet1','A2');
24 -   end
25 -   clear;
26 -   clc;
27 -   end
28 -

```

Figure 3.16: Example code for WWLLN data.

CHAPTER 4

RESULTS AND DISCUSSION

4.1 INTRODUCTION

This chapter presents about the results obtained from the EFM, FA system, weather radar and WWLLN. Based on the results, analyze the type of lightning flashes, electric field change, number of thunderstorms, rainfall rate, radar reflectivity and location of lightning events occurred. After that, correlate all the data and discuss about it.

4.2 COMPARISON BETWEEN EFM, FA SYSTEM, WEATHER RADAR AND WWLLN

4.2.1 OCCILATION OF AN ELECTRIC FIELD

To transfer data from the field mill to remote computers, the EFM display software attempted to establish and maintain a network link with them. Depending on the weather, differences in atmospheric energy data can be observed in a variety of ways. This software can be used to view real-time electric field data in relation to an alarm annunciator, amplitude range selector, time range selector, and other geographical features of interest [62]. The history graph and the current field reading can both be viewed in the EFM display software.

In terms of the area for which the ensuing lightning warnings were valid, EFM had a limited range. This range was influenced by elements such as orography, surface form, nearby structures, and so on, and was determined by the precise position [42]. The EFM sensor was located at Universiti Teknikal Malaysia Melaka (UTEM), which was located at N 2°18'59.04" latitude and E 102°19'15.1176" longitude in Peninsular Malaysia. The atmospheric electric

field data will then be compared to lightning data acquired from the FA system and radar data using MATLAB software and numerical method analysis.

Based on Figure 4.1, the graph depicted the oscillations of an electric field variance measured during 4am to 2pm on 11 August 2020 at Malacca. There were two storms occurred during these 10 hours. The first storm was happened in 05:00:00 to 06:59:59, by then the second storm was happened in 07:00:00 to 14:00:00. The second storm happened in quick succession. Besides that, according to Figure 4.1, the oscillations of first storm were very small which the reading of electric field change was 0.75kV/m, that's mean the first storm was occurred not far from the location of the EFM sensor (UTeM). Apart from that, when compared to the rest of the readings obtained on that day, the highest reading of electric field change was 9.8kV/m with the lightning detection being away from the position of the EFM sensor (UTeM).

Thunderstorms had a dipolar charge structure with a negative polarity electric field. It also resulted in the CG flash's significant negative discharge and active phase [63]. In fine weather, the electric field strength was negatively connected with atmospheric conductivity, but positively correlated with aerosol content, vapor, temperature, and other weather variables [64].

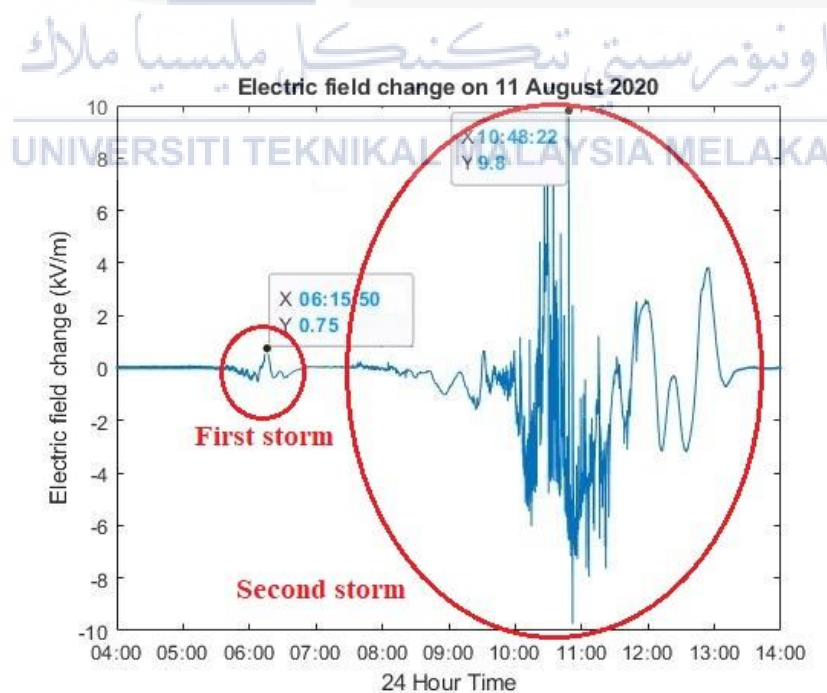


Figure 4.1: Electric field at the ground on 11 August 2020.

4.2.2 ANALYSIS OF TYPE OF LIGHTNING FLASHES

In this research, FA system was chosen because FA system is a well-known and accurate lightning measurement. The FA data was used to classify the types of lightning flashes such as Cloud-to-Ground (CG), Intra-Cloud (IC) and Narrow Bipolar Event (NBE) based on the waveform by using the Picoscope software.

Based on Figure 4.2, a total of 1024 lightning flashes were detected by FA system in this research. The highest occurrence of type of lightning flashes on 11 August 2020 in Malacca was IC (436) and the lowest occurrence of type of lightning flashes on 11 August 2020 in Malacca was negative NBE around 6. However, a total of 337 CG lightning events were detected which consisted of 310 were negative CG, and the rest of flashes were positive CG. Malaysia is a tropical country on the equator's edge. According to the Malaysian Meteorological Services, it had a lot of lightning and thunderstorms events with an average of 200 thunder days per year [65]. As discussed by Chin Leong Wooi et.al [66], in Malaysia, only 14% to 31% from total CG lightning events were positive lightning, the rest of CG lightning events were negative lightning which was 82%. This proved that positive lightning is very rare occurred in Malaysia and majority of CG lightning events are negative lightning.

Besides that, Figure 4.3 showed the number of return stroke that detected by FA system on 11 August 2020 in Malacca. Based on Figure 4.3, there were 337 CG flashes detected and the maximum number of return stroke that detected by FA system was 14. However, majority CG flashes consisted of 1 or 2 return strokes which were 205 and 32 respectively. Only minority of samples had 13 or 14 return strokes. In addition, Figure 4.4 showed the expanded view of fast field signal that captured by FA system at 10:06:48. Based on Figure 4.4, there were 14 return strokes are detected by FA system which the range of duration of each return stroke was between $30\mu\text{s}$ to $80\mu\text{s}$.

Moreover, Figure 4.5 showed the flash rate during 04:00:00 to 14:00:00 on 11 August 2020 in Malacca. During this period, the maximum flash rate was 218 flashes per 10 minutes. The evolution of flash rate in Figure 4.5 was not uniformly which the flash rate rose slightly until flash rate become 26 flashes per 10 minutes at 05:50:01 then declined slightly. After 07:30:00, it started to become very unstable. It repeated to increase and decrease rapidly around

07:30:00 to 12:00:00. Afterwards, the flash rate was beginning of a weakening period from peak maturity before it moved out of the analysis domain.

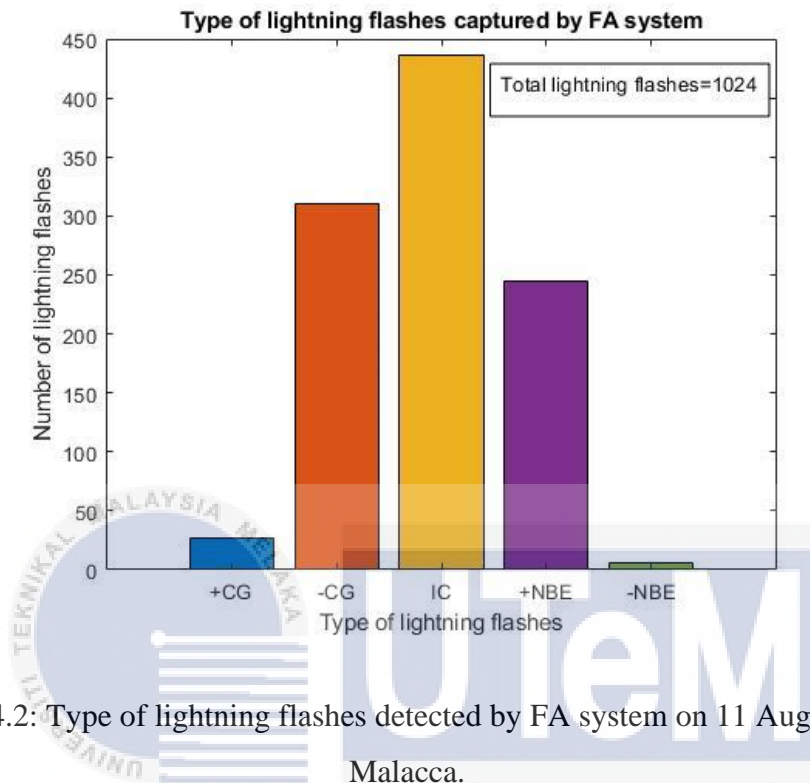


Figure 4.2: Type of lightning flashes detected by FA system on 11 August 2020 in Malacca.

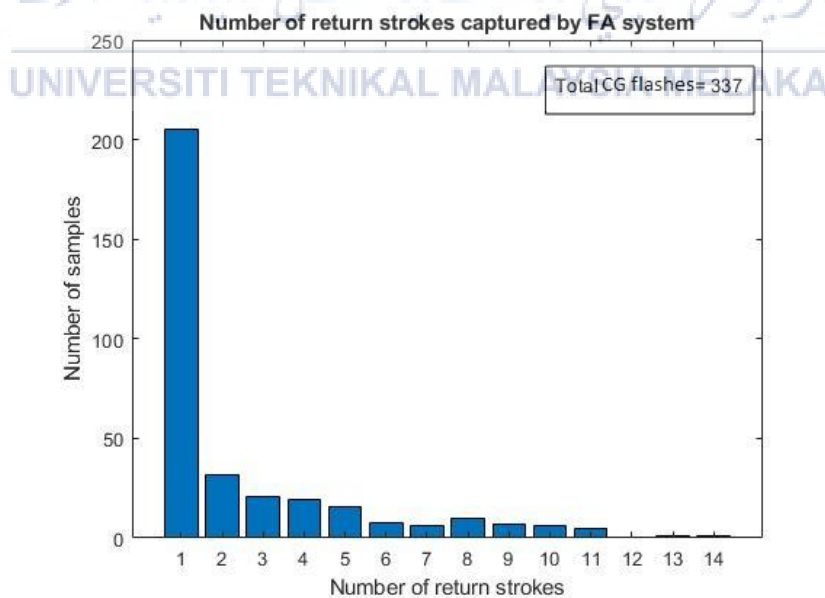


Figure 4.3: Number of return strokes detected by FA system on 11 August 2020 in Malacca.

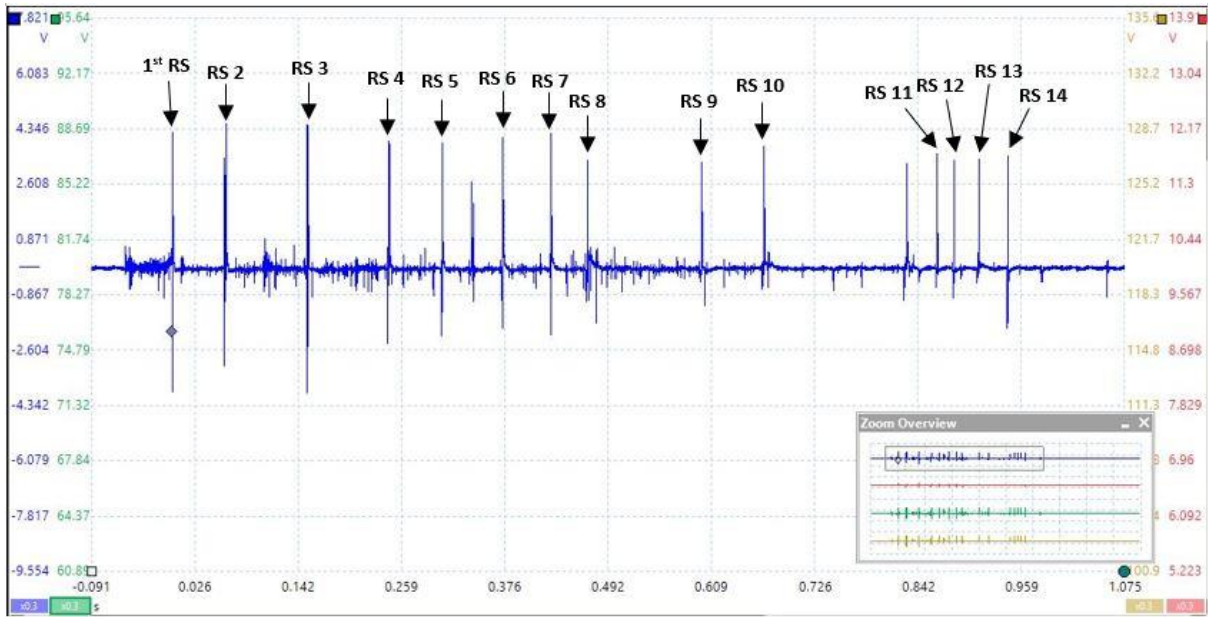


Figure 4.4: The expanded view of fast field signal at 10:06:48.

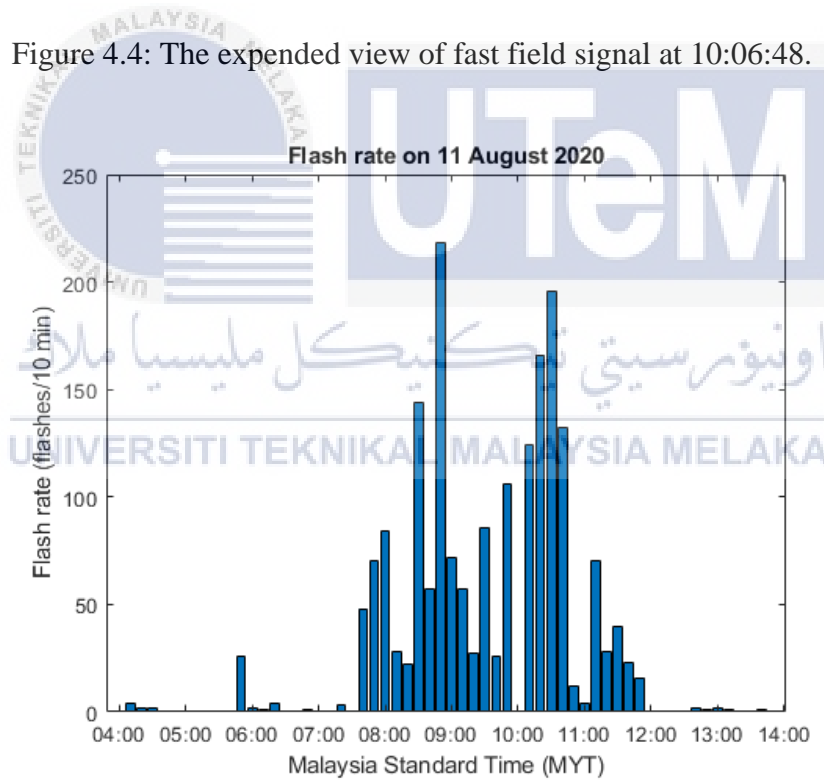


Figure 4.5: Evolution of flash rate per 10 minutes on 11 August 2020 in Malacca.

4.2.3 ANALYSIS OF RADAR DATA

The radar data in CAPPI format was generated in every 10 minutes. Because of its capacity to display high-resolution images that can be easily studied, CAPPI was chosen. The radar can be used to determine the rate of rainfall as well as radar reflectivity. The rate of rainfall cannot be directly detected by weather radar. Only by relating the radar reflectivity, Z (mm^6/m^3) to the rainfall rate, R (mm/h) can be determined. Rainfall rates were proportional to the volume of raindrops, yet reflectivity was related to the drop diameter divided by the sixth power [54].

Generally, light rain was defined as reflectivity values of less than 35 dBZ; moderate rain was defined as reflectivity values of 35 to 50 dBZ; and heavy rain was defined as reflectivity values of more than 50 dBZ. Reflectivity values greater than or equal to 55 dBZ were typically used to identify hail [52].

Based on the Figure 4.6, the maximum rainfall rate was reached 50mm/h which around 9:30:00 to 11:00:00. At similar time, the radar reflectivity data revealed that the second storms reached maximum values at 50dBZ. Therefore, there was heavy rain when around 9:30:00 to 11:00:00. Besides that, the movement and location of rainfall also can be observed from the radar data in CAPPI format. For the first storm that occurred during 5:00:00 to 7:00:00, the location of the rainfall was moved from Klebang to Ayer Keroh after that to Alor Gajah. Moreover, for the second storm that occurred during 7:00:00 to 14:00:00, the location of the rainfall was started moved from Masjid Tanah and then whole area of Malacca.

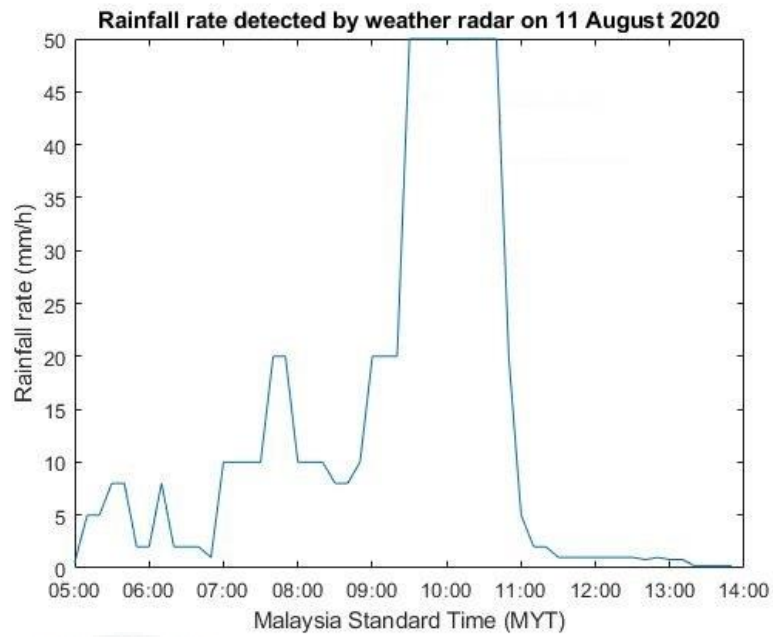


Figure 4.6: Rainfall rate recorded by weather radar on 11 August 2020.

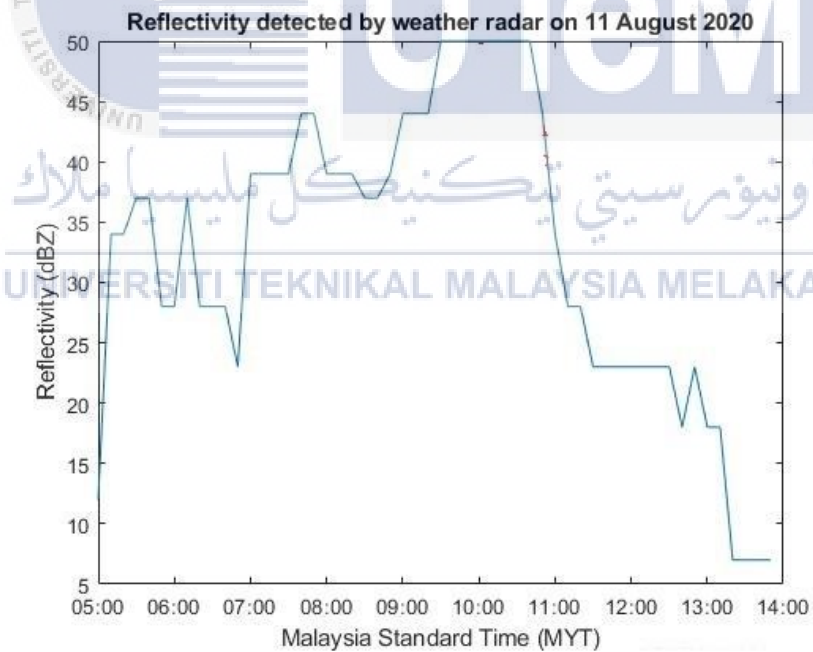

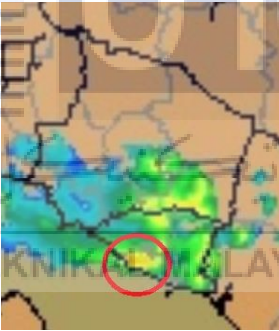

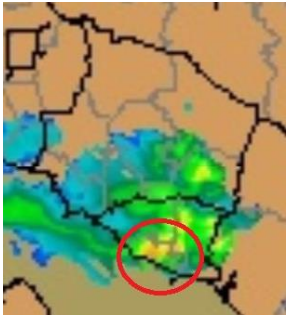


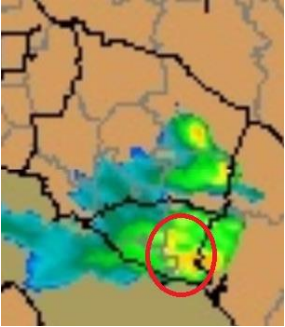



Figure 4.7: Radar reflectivity recorded by weather radar on 11 August 2020.

Table 4.1: Maximum rainfall rate detected by weather radar on 11 August 2020 in Malacca.

| 24 Hour Time | Radar data | Rainfall rate (mm/h) |
|--------------|---|----------------------|
| 09:30:07 |  | 20-50 |
| 09:40:08 |  | 20-50 |
| 09:50:07 |  | 20-50 |

| | | |
|----------|---|-------|
| 10:00:08 |  | 20-50 |
| 10:10:04 |  | 20-50 |
| 10:20:07 |  | 20-50 |

| | | |
|----------|--|-------|
| 10:30:09 |  | 20-50 |
| 10:40:14 |  | 20-50 |



اونيورسيتي تېكنيكل ماليسيا ملاك

UNIVERSITI TEKNIKAL MALAYSIA MELAKA

4.2.4 WORLD WIDE LIGHTNING LOCATION NETWORK (WWLLN) DATA

The world wide lightning location network (WWLLN) data consisted of details of lightning strikes, estimated energy, and detection efficiency fields. Malacca is located at latitude 2.196 (2°11'45.6" N) and longitude 102.2405(102°14'25.8" E). Therefore, the area of observation was set to whole area of Malacca which the range of latitude was 2 to 2.5, and the range of longitude was 101.9 to 102.6. Figure 4.8 shows the location of lightning strike that detected by WWLLN on 11 August 2020. Based on Figure 4.8, majority of lightning strikes were located at Alor Gajah and Melaka Tengah. However, only minority of lightning strikes were located at Jasin.

Moreover, energy of lightning strike that was detected by WWLLN as shown in Figure 4.9. Based on Figure 4.9, the highest energy of lightning strike that detected by WWLLN at 10:51:51 was 14.526kJ. The energy of lightning strike that detected by WWLLN around 09:30:00 to 11:30:00 was in the range of 0.08 to 3kJ. The lowest energy of lightning strike on 11 August 2020 was 0.076kJ.

Besides that, Figure 4.10 displayed the evolution of strike rate and Table 4.2 recorded number of lightning strikes detected by WWLLN on 11 August 2020. Based on the Figure 4.10, the maximum strike rate was 70 strikes per 10 minutes which occurred at 10:50:07. The strike rate was unstable until it reached the maximum strikes rate, but after that it declined sharply. Moreover, based on Table 4.2, a total of 338 lightning strikes were detected by WWLLN on 11 August 2020. Moreover, the highest number of lightning strike was 225 which detected by WWLLN during 10:00:00 to 10:59:59. While the lowest number of lightning strike was 5 which detected by WWLLN during 07:00:00 to 07:59:59.

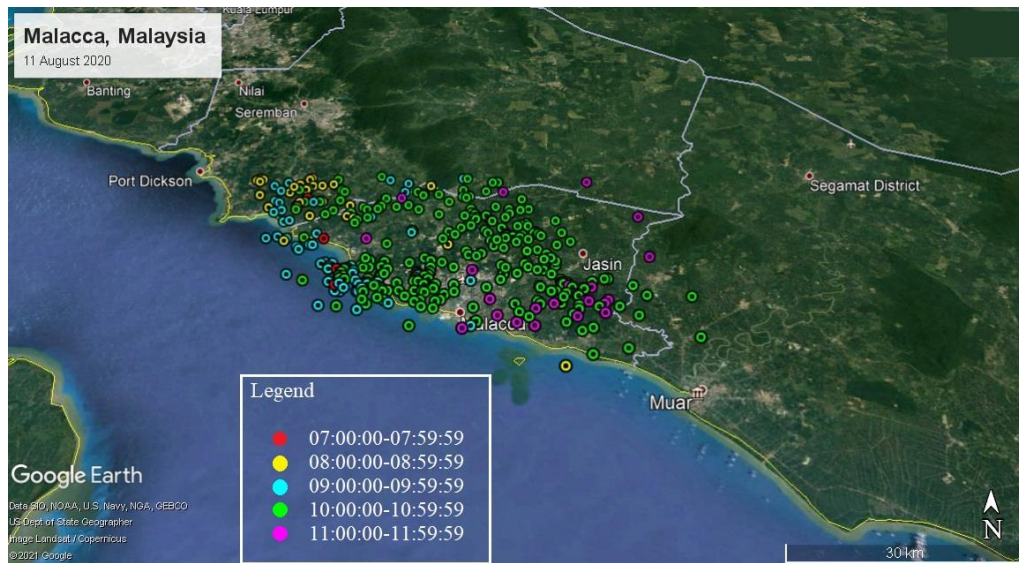


Figure 4.8: The location of lightning strike detected by WWLLN.

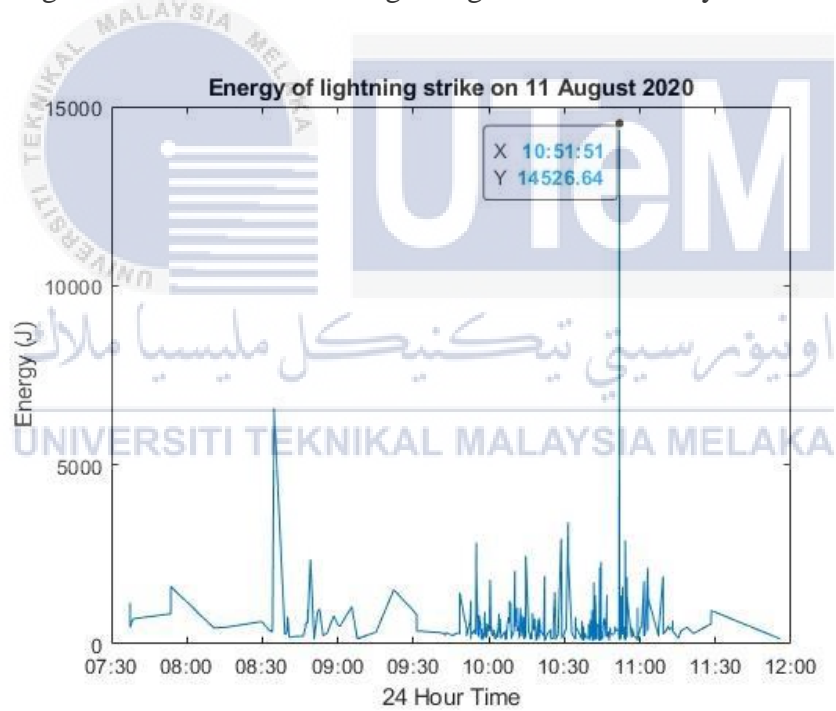


Figure 4.9: Energy of lightning strike detected by WWLLN on 11 August 2020 in Malacca.

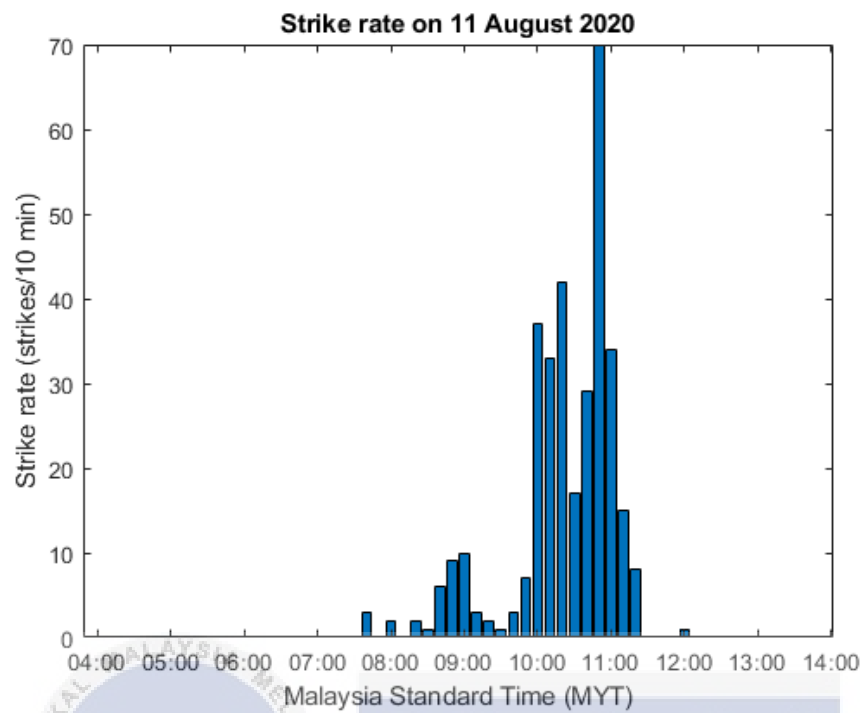


Figure 4.10: Evolution of strike rate on 11 August 2020 on Malacca.

Table 4.2: Number of lightning strike detected by WWLLN on 11 August 2020.

| Malaysia Standard Time (MYT) | Number of lightning strike |
|------------------------------|----------------------------|
| 07:00:00-07:59:59 | 5 |
| 08:00:00-08:59:59 | 28 |
| 09:00:00-09:59:59 | 53 |
| 10:00:00-10:59:59 | 225 |
| 11:00:00-11:59:59 | 27 |
| Total | 338 |

4.2.5 CORRELATION BETWEEN ELECTRIC FIELD, LIGHTNING FLASHES, RAINFALL RATE AND WWLLN

Based on results obtained from EFM sensor which as shown in Figure 4.1, there were 2 storms that occurred on 11 August 2020 in Malacca. The first storm was happened around 05:00:00 to 06:59:59 and second storm was happened around 07:00:00 to 14:00:00. The maximum electric field change for the first storm was 0.75kV/m while the second storm had reached the maximum electric field change which was 9.8kV/m.

A total of 33 lightning flashes were detected from FA system during the first storm occurred as shown in Figure 4.10. From these 33 lightning flashes, the highest occurrence of lightning flashes during the first storm was positive NBE (21), the lowest occurrence of lightning flashes was negative NBE (1), and there was no any flash was positive CG. The flash rate during first storm occurred was not stable. The flash rate in first storm was quite low and the highest flash rate was from 26 flashes per 10 minutes.

Besides that, the maximum rainfall rate that detected by weather radar during the first storm happened was 8mm/h. At similar time, the radar reflectivity data revealed that the first storm reached maximum values at 37dBZ. Based on the value of rainfall rate and radar reflectivity, light rain was occurred during the first storm. During the first storm occurred, the rainfall was moved from Klebang to Ayer Keroh after that to Alor Gajah. Based on the results obtained from WWLLN, there was no lightning strike detected during the period of first storm happened.

Moreover, there are 980 lightning flashes detected by FA system during the second storm occurred as shown in Figure 4.11. Majority of type of lightning flashes during second storm was IC around 429 while the minority of type of lightning flashes during second storm was negative NBE around 4. The second storm had reached the maximum flash rate which was 218 flashes per 10 minutes. Then, after 11:30:00 which was the late stage of second storm, the flash rate dropped until the lowest which was 0 flashes per 10 minutes.

In addition, the type of lightning flashes that detected by FA system before and after the highest electric field as shown in Figure 4.12. According to Figure 4.12, the majority type of lightning flashes detected was negative CG which before 30 minutes and during the highest

electric field reached. Although after 30 minutes the highest electric field reached, there were same number of lightning flashes in IC and negative CG. The minority of type of lightning flashes was negative NBE.

However, the maximum rainfall rate that detected by weather radar during the second storm happened was 50mm/h. In the meantime, the radar reflectivity data revealed that the second storm reached maximum values at 50dBZ. Based on the value of rainfall rate and radar reflectivity, heavy rain was occurred during the second storm. During the second storm occurred, the rainfall was started moved from Masjid Tanah and then whole area of Malacca. Based on the results obtained from WWLLN, a total of 338 lightning strikes were detected during the period of second storm happened. The highest number of the lightning strikes were detected during 10:00:00 to 10:59:59 which was 225 strikes. The highest strike rate was 70 strikes per 10 minutes during the peak hour (10:00:00 to 10:59:59). The area of lightning strikes detected was almost covered the whole area of Malacca.

In additional, Figure 4.13(a) and Figure 4.13(b) showed the active region for lightning strike and highest reflectivity by weather radar and WWLLN. Based on Figure 4.13(b), the highest reflectivity value that indicated by the intensity of its color gauge in CAPPI data. The region where the thunderstorm was reported to have occurred was covered by the active region. Moreover, the location of lightning strikes that detected by WWLLN were focused on the active region also.

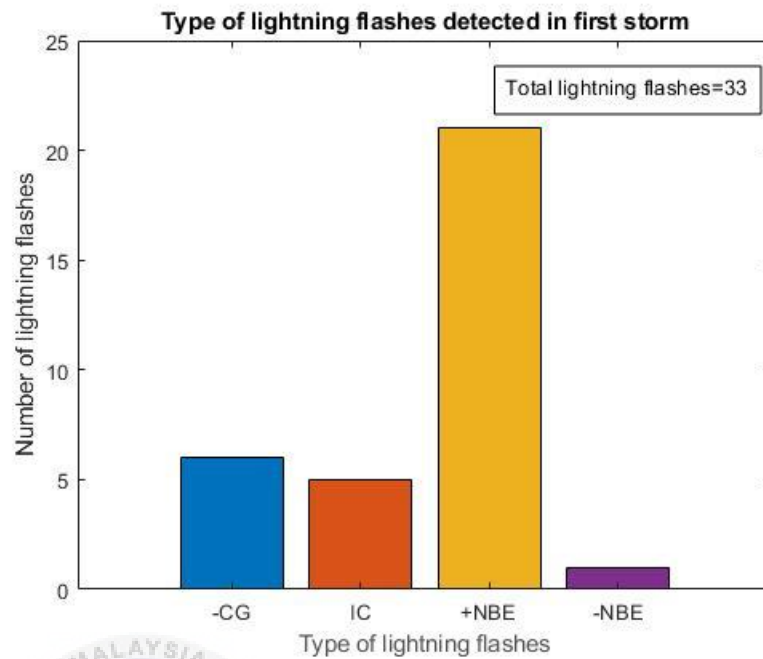


Figure 4.10: Type of lightning flashes detected by FA system from 05:00:00 to 06:59:59 (first storm).

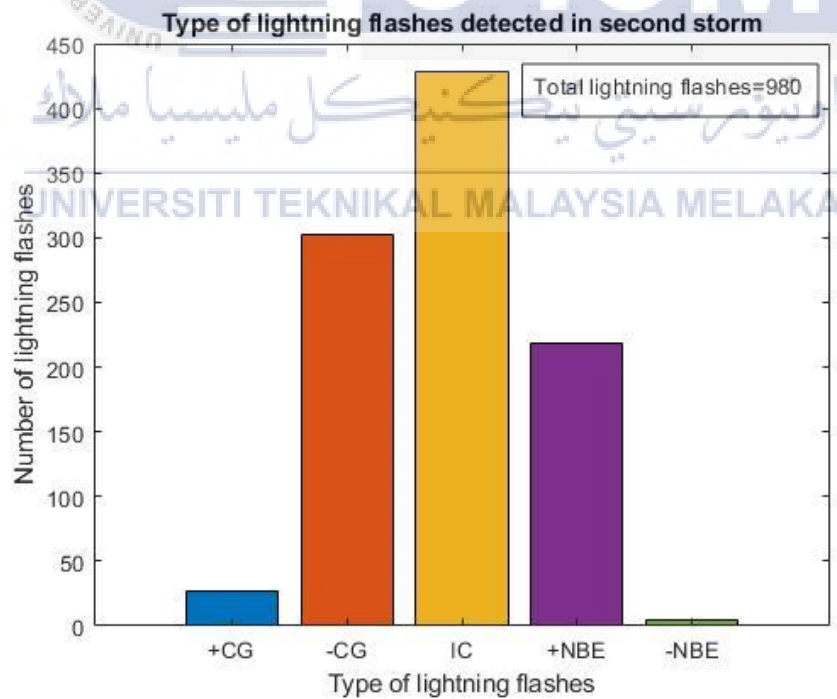


Figure 4.11: Type of lightning flashes detected by FA system from 07:00:00 to 14:00:00 (second storm).

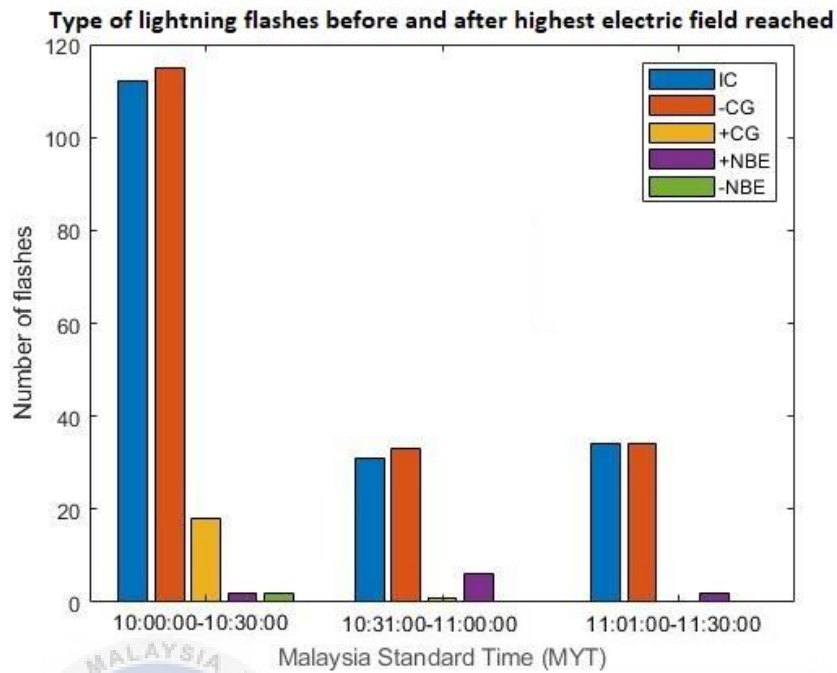


Figure 4.12: Type of lightning flashes before and after 10:48:22 (highest electric field).

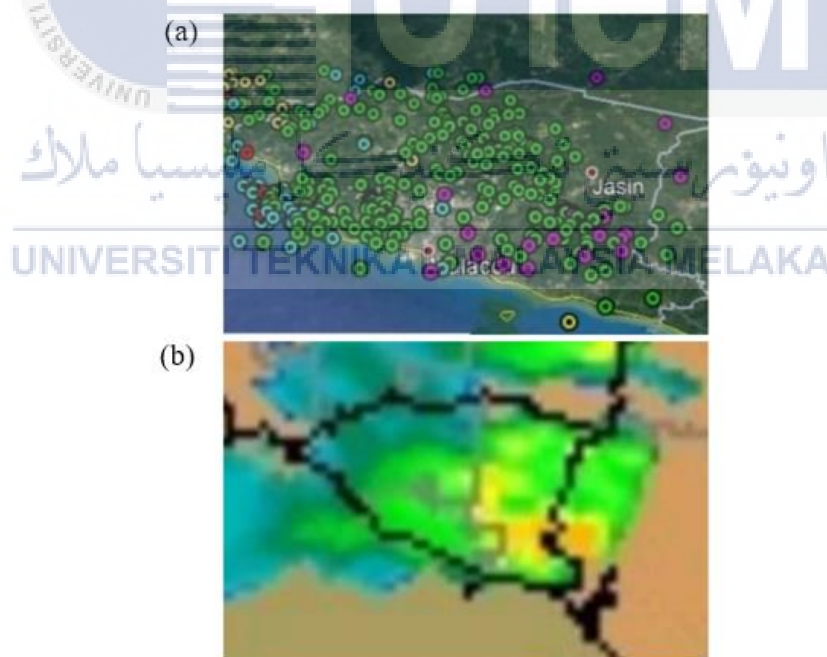


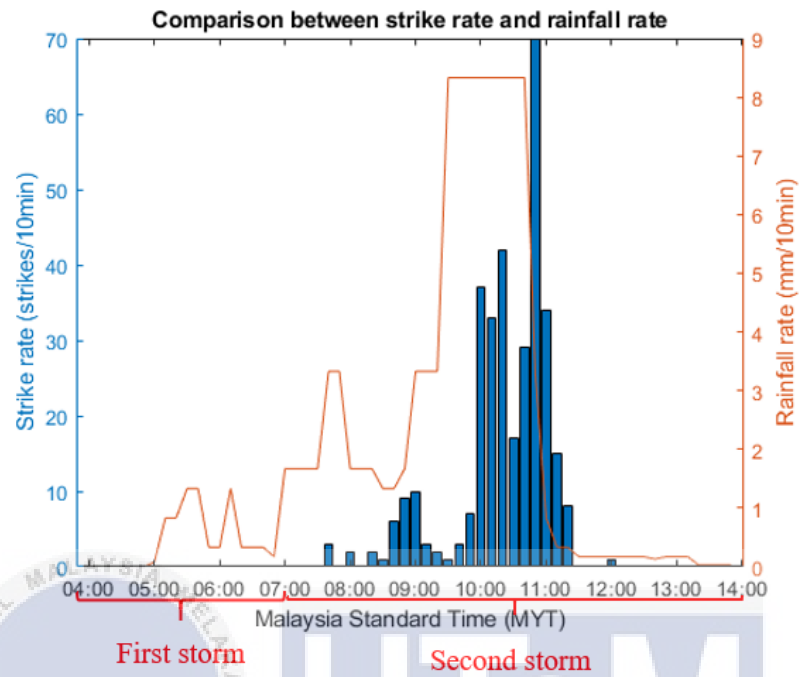
Figure 4.13(a): Location of lightning strike detected by WWLLN.

Figure 4.13(b): Active region for highest reflectivity detected by weather radar.

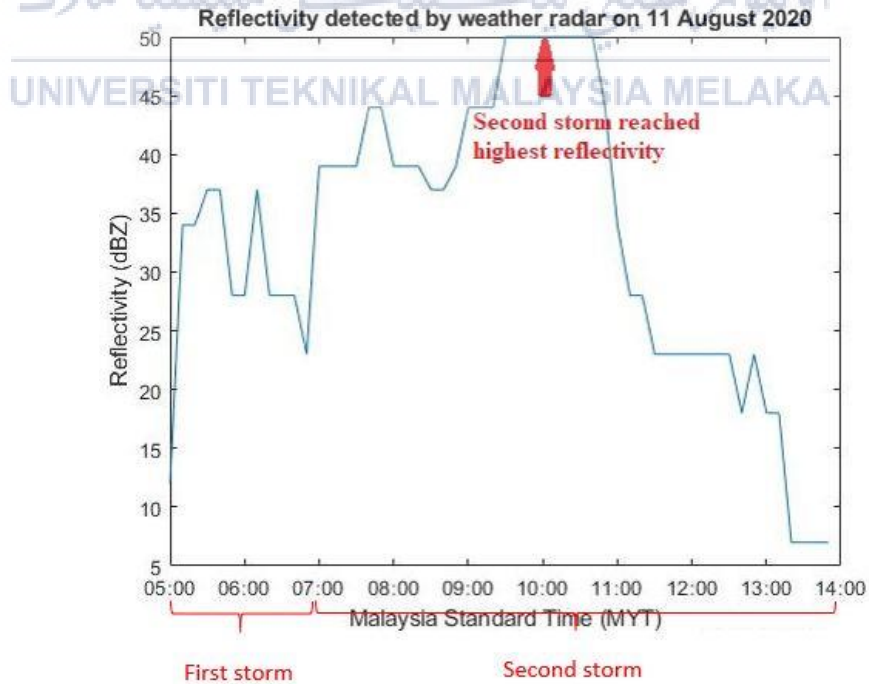
Table 4.3: Comparison between analysis obtained by EFM, weather radar and WWLLN.

| | |
|------------|---|
| <p>No.</p> | <p>Comparison between analysis obtained by EFM sensor, weather radar and WWLLN</p> |
| <p>1</p> | <p>Electric field change on 11 August 2020</p> <p>The graph plots Electric field change (kV/m) on the y-axis (ranging from -10 to 10) against 24 Hour Time on the x-axis (ranging from 04:00 to 14:00). Two specific points are highlighted with red circles and callouts: 'First storm' at X 06:15:50, Y 0.75, and 'Second storm' at X 10:48:22, Y 9.8. The second storm shows a much larger amplitude and more complex oscillation compared to the first.</p> |
| <p>2</p> | <p>Comparison between flash rate and rainfall rate</p> <p>The graph plots Flash rate (flashes/10min) on the left y-axis (0 to 250) and Rainfall rate (mm/10min) on the right y-axis (0 to 9) against Malaysia Standard Time (MYT) on the x-axis (04:00 to 14:00). Blue bars represent the flash rate, and an orange line represents the rainfall rate. Two storm periods are marked with red brackets: 'First storm' from approximately 05:00 to 07:00, and 'Second storm' from approximately 08:00 to 11:00. The second storm shows a significant peak in both flash rate (around 220 flashes/10min) and rainfall rate (around 8 mm/10min).</p> |

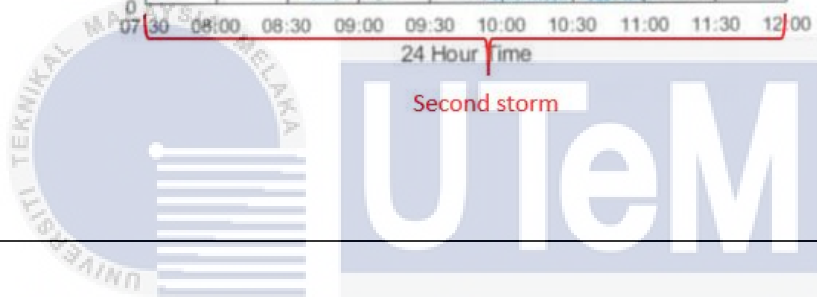
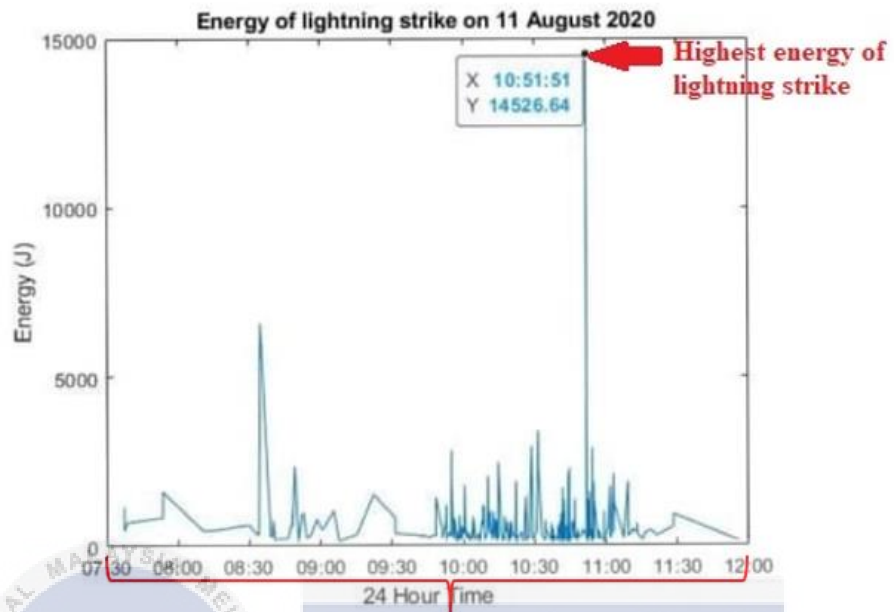
3



4



5



اونيورسيتي تيكنيكل مليسيا ملاك
UNIVERSITI TEKNIKAL MALAYSIA MELAKA

Table 4.4: Summary of first and second storm on 11 August 2020 in Malacca.

| | First storm | Second storm |
|--|--|---|
| Duration happened storm (Malaysia Standard Time) | 05:00:00 to 06:59:59 | 07:00:00 to 14:00:00 |
| Highest electric field change (kV/m) | 0.75 | 9.80 |
| Total number of lightning flashes | 33 | 980 |
| Majority type of lightning flashes | Positive NBE | IC |
| Maximum flash rate (flashes/10min) | 26 | 218 |
| Maximum rainfall rate (mm/h) | 8 | 50 |
| Maximum radar reflectivity (dBZ) | 37 | 50 |
| Intensity of rainfall | Light rain | Heavy rain |
| Movement of rainfall | Klebang to Ayer Keroh after that to Alor Gajah | Masjid Tanah and then whole area of Malacca |
| Total number of lightning strikes (WWLLN) | - | 338 |
| Maximum strike rate (strikes/10min) | - | 70 |
| Peak hour that lightning strikes had detected (Malaysia Standard Time) | - | 10:00:00 to 10:59:59 |

CHAPTER 5

CONCLUSION AND FUTURE WORK

5.1 CONCLUSION

First and foremost, the project has fulfilled the two objectives which have proposed early in this report. The types of lightning flashes on 11 August 2020 in Malacca have been classified and the results obtained from EFM sensor, FA system, weather radar and WWLLN has been correlated.

In addition, there are 2 storms detected by EFM sensor on 11 August 2020 in Malacca which those storms happened during 05:00:00 to 06:59:59 and 07:00:00 to 14:00:00 respectively. A total of 1024 lightning flashes detected by FA system and majority of them is IC around 436. Then, the maximum number of return strokes detected is 14 which occurred at 10:06:48.

In a nutshell, there are 33 lightning flashes detected and most of them are positive NBE (21) in first storm. Based on the value of rainfall rate and reflectivity, light rain is happened in first storm. For the second storm, there are 980 lightning flashes detected and IC has the highest occurrence which is 429. According to value of rainfall rate and reflectivity, heavy rain is happened in second storm. Besides that, WWLLN has detected majority of lightning strikes are concentrated at Alor Gajah and Melaka Tengah. A total of 338 lightning strikes are detected by WWLLN in second storm and majority of them occurred during the peak hour (10:00:00 to 10:59:59).

5.2 RECOMMENDATIONS FOR FUTURE WORK

According to the results obtained in this project, there are 2 storms have detected on 11 August 2020 in Malacca. Majority of type of lightning flashes detected in first storm and second storm is positive NBE and IC respectively. Based on the value of rainfall rate and reflectivity detected by weather radar, we can conclude that light rain is happened during first storm and moderate rain is happened during second storm. Unfortunately, there are some weaknesses and limitation can be improve in lightning analysis.

One of the weaknesses is the EFM sensor that used to collect the lightning data in this project. The sensitivity of field mills (and hence lightning range estimates) is extremely dependent on site conditions and impossible to calibrate without specialist expertise and equipment. BTD series is suggested to replace the EFM sensor to detect atmospheric electric field. The BTD series used specialized signals to reduce false alarms, such as strongly charged precipitation or strong E-field fluctuations (not absolute strength).

Moreover, the accuracy of classification of type of lightning flashes is also one of the weaknesses in this project. In this project, Picoscope 6 is used to observe the waveform and classify the type of lightning flashes. Due to there are too many different and complicated patterns of each type of lightning flashes, it increased the difficulties to classify the type accurately if the researcher did not have several years of experiences and understanding in this field. Therefore, invention of one software to help the researcher to classify the type of lightning flashes accurately.

Last but not least, the value of rainfall rate obtained by using weather radar is just an estimation based on the color gauge. Weather radar is not as “local” as a rain gauge and errors are created by terrain in several places. Rain gauge is suggested to replace the weather radar. There are several reasons replaced weather radar to rain gauge such as rain gauge is the instrument that is simple and inexpensive, and localized data that is more suited to catchment areas.

REFERENCES

- [1] H.Z. Abidin, R. Ibrahim (January 2004). *Thunderstorm day and ground flash density in Malaysia*. Retrieved from https://www.researchgate.net/publication/4145830_Thunderstorm_day_and_ground_flash_density_in_Malaysia
- [2] Chuntao Liu, Daniel J, Edward J. Zipser, Kevin Kronfeld, Roy Robertson (27 March 2012). *Relationship between lightning flash rates and radar reflectivity vertical structures in thunderstorms over the tropics and subtropics*. Retrieved from <https://agupubs.onlinelibrary.wiley.com/doi/full/10.1029/2011JD017123>
- [3] Norbayah Yusop, Mohd Riduan Ahmad et.al (26 November 2019). *Seasonal Analysis of Cloud-To-Ground Lightning Flash Activity in the Western Antarctica*.
- [4] Hwee Geem Chan, Amir Izzani bin Mohamed (2 August 2018). *Investigation on the occurrence of positive cloud to ground (+CG) lightning in UMP Pekan*.
- [5] Norbayah Yusop, Mohd Riduan Ahmad et.al (8 May 2019). *Cloud-to-Ground lightning observations over the Western Antarctic region*.
- [6] Mohd Riduan Ahmad, Dinesh Periannan Muhammad Haziq Mohammad Sabri et.al (2017). *Emission Heights of Narrow Bipolar Events in a Tropical Storm over the Malacca Strait*.
- [7] Chin-Leong Wooi, Abdul-Malek, Z. Ahmad et.al (2016). *Statistical analysis of electric field parameters for negative lightning in Malaysia*. *Journal of Atmospheric and Solar-Terrestrial Physics*, 146, 69-80. Retrieved from <https://sci-hub.do/https://www.sciencedirect.com/science/article/abs/pii/S136468261630133X?via%3Dihub>
- [8] Wooi, C. L., Abdul-Malek, Z., Ahmad, N. A., Mokhtari, M., & Khavari, A. H. (2016). *Cloud-to-Ground Lightning in Malaysia: A Review Study*. *Applied Mechanics and Materials*, 818, 140-145. Retrieved from <https://sci-hub.do/https://www.scientific.net/amm.818.140>
- [9] Chin-Leong Wooi, Zulkarnain Malek et.al (2016). *Statistical Analysis on Preliminary Breakdown Pulses of Positive Cloud-to-Ground Lightning in Malaysia*. Retrieved from https://www.researchgate.net/profile/Mehrdad_Mokhtari2/publication/299549978_Statistical_Analysis_on_Preliminary_Breakdown_Pulses_of_Positive_Cloud-to-Ground_Lightning_in_Malaysia/links/57257fdd08aee491cb3aa266.pdf
- [10] Salimi, B., Mehranzamir, K., & Abdul-Malek, Z. (2013). *Statistical analysis of lightning electric field measured under Malaysian condition*. *Asia-Pacific Journal of Atmospheric Sciences*, 50(2), 133-137. Retrieved from <https://sci-hub.do/https://link.springer.com/article/10.1007%2Fs13143-014-0002-0>
- [11] RMetS (2019). *Types of Lightning*. Retrieved from <https://www.theweatherclub.org.uk/node/431>
- [12] NSSL. *Severe Weather 101- Lightning*. Retrieved from <https://www.nssl.noaa.gov/education/svrwx101/lightning/types/>
- [13] DAN ROBINSON. *Lightning Types and Classifications*. Retrieved from <https://stormhighway.com/types.php>
- [14] M.R. Ahamad, M.R.M. Esa et.al (17 March 2015). *Latitude dependence of narrow bipolar pulse emissions*.
- [15] Smith, D. A. et al. *A distinct class of isolated intracloud lightning discharges and their associated radio emissions*. *J. Geophys. Res.* 104, 4189-4212 (1999).

- [16] The Alabama Weather Blog (2020). *Different Types of Lightning*. Retrieved from <https://www.alabamawx.com/?p=173831#:~:text=Cloud%2Dto%2Dair%20lightning%20is,that%20are%20opposite%20charges%20and>
- [17] Cooray, V. (2015). *An Introduction to Lightning*. doi:10.1007/978-94-017-8938-7
- [18] Saba MF, Cummins KL, Warner TA, Krider EP, Campos LZS, Ballarotti MG, Pinto O Jr, Fleenor SA (2008) Positive leader characteristics from high-speed video observations. *Geophys Res Lett* 35:L07802. doi:10.1029/2007GL033000
- [19] Chilingarian, A., Khanikyants, Y., Mareev, E., Pokhsraryana, D., Rakov, V. A., & Soghomonyan, S. (2017). *Types of lightning discharges that abruptly terminate enhanced fluxes of energetic radiation and particles observed at ground level*. *Journal of Geophysical Research: Atmospheres*, 122(14), 7582–7599. doi:10.1002/2017jd026744
- [20] Wu, T., Yoshida, S., Ushio, T., Kawasaki, Z., & Wang, D. (2014). *Lightning-initiator type of narrow bipolar events and their subsequent pulse trains*. *Journal of Geophysical Research: Atmospheres*, 119(12), 7425–7438. doi:10.1002/2014jd021842
- [21] Jiaquan Wong, QiJun Huang et.al (2020). *Classification of VLF/LF Lightning Signals Using Sensors and Deep Learning Methods*. Retrieved from <https://www.ncbi.nlm.nih.gov/pmc/articles/PMC7070770/>
- [22] Cummins, K. L., & Murphy, M. J. (2009). *An Overview of Lightning Locating Systems: History, Techniques, and Data Uses, With an In-Depth Look at the U.S. NLDN*. *IEEE Transactions on Electromagnetic Compatibility*, 51(3), 499–518. doi:10.1109/temc.2009.2023450
- [23] Stones, J. (2003). *Power Quality*. *Electrical Engineer's Reference Book*, 43–1–43–9. doi:10.1016/b978-075064637-6/50043-5
- [24] Browne B J, Gaesch WR (1992). *Electrical injuries and lightning*. *Emerg Med Clin North Am* 10:211-229.
- [25] Langley RL, Ounn KA (1991). *Lightning fatalities in North Carolina*. *N C Meg J* 52:281-284.
- [26] Jan W.van Wagendok, Daniel R. Cayan (2008). *Temporal and Spatial Distribution of Lightning Strikes in California in Relation to Large-Scale Weather Patterns*. Retrieved from <https://doi.org/10.4996/fireecology.0401034>
- [27] Uman, M.A. (1987). *The lightning discharge*. Dover Publications, Mineola, New York, USA
- [28] Rakov, V. A., M. A. Uman (2003). *Lightning: Physics and Effects*. Cambridge Univ. Press, New York.
- [29] Amitabh Nag, Vladimir A. Rakov (8 January 2008). *Pulse trains that are characteristics of preliminary breakdown in cloud-to-ground lightning but are not followed by return stroke pulses*. *JOURNAL OF GEOPHYSICAL RESEARCH*, VOL. 113, D01102, doi:10.1029/2007JD008489.
- [30] M.J. Murphy, et al (1984-2012). *Lightning charge analyses in small Convection and Precipitation Electrification (CaPE) experiment storms*. *Journal of Geophysical Research: Atmospheres*. vol. 101, pp. 29615-29626, 1996.
- [31] Z. A. Baharudin, N. A. Ahmad, M. Fernando, V. Cooray, and J. Mäkelä (2012). *Comparative study on preliminary breakdown pulse trains observed in Johor, Malaysia and Florida, USA*. *Atmospheric research*, vol. 117, pp. 111-121.
- [32] Clarence, N.D., Malan, D.J. (1957). *Preliminary discharge processes in lightning flashes to ground*. *Quarterly Journal of the Royal Meteorological Society* 83, 161–172.

- [33] Wooi, C.-L., Abdul-Malek, Z., Ahmad, N. A., & Mokhtari, M. (2015). *Characteristic of preliminary breakdown preceding negative return stroke in Malaysia*. IEEE Conference on Energy Conversion (CENCON). doi:10.1109/cencon.2015.7409523
- [34] C. Schumann, et al. (2013). *Electric fields changes produced by positives cloud-to-ground lightning flashes*. Journal of Atmospheric and Solar-Terrestrial Physics, vol. 92, pp. 37-42.
- [35] A. Nag and V.A. Rakov (2009). *Electric field pulse trains occurring prior to the first stroke in negative cloud-to-ground lightning*. Electromagnetic Compatibility, IEEE Transactions on, vol. 51, pp. 147-150.
- [36] National Weather Service (2021). *Understanding Lightning: Initiation of a Stepped Leader*. Retrieved from <https://www.weather.gov/safety/lightning-science-initiation-stepped-leader>
- [37] Schonland BFJ (1956). *The lightning discharge*. Handb Phys 22:576–628
- [38] Wang D, Takagi N, Watanabe T, Rakov VA, Uman MA (1999). *Observed leader and return stroke propagation characteristics in the bottom 400 m of rocket triggered lightning channel*. J Geophys Res 104:14369–14376
- [39] Saba MMF, Ballarotti MG, Pinto O (2006). *Negative cloud-to-ground lightning properties from high-speed video observations*. J Geophys Res 111: D03101
- [40] Yves-Bernard Andre, Guillaume Mejean (November 2008). *Progress towards lightning control using lasers*. Retrieved from https://www.researchgate.net/publication/237218507_Progress_towards_lightning_control_using_lasers
- [41] Boltek Corporation (2016). *Lightning Detection Systems*. Retrieved from <https://www.boltek.com/EFM100-SS-09112016.pdf>
- [42] De Bilt (2013). *Static electricity measurements for lightning warnings-an exploration*.
- [43] Martin J. Murphy, Ronald L Holle, Nicholas W S Demetriades (3 June 2014). *CLOUD-TO-GROUND LIGHTNING WARNINGS USING ELECTRIC FIELD MILL AND LIGHTNING OBSERVATIONS*. Retrieved from [\(PDF\) 6.5 CLOUD-TO-GROUND LIGHTNING WARNINGS USING TOTAL LIGHTNING MAPPING AND ELECTRIC FIELD MILL OBSERVATIONS \(researchgate.net\)](#)
- [44] Z. A. Baharudin, Noor Azlinda Ahmad et.al (14 December 2013). *Negative cloud-to-ground lightning flashes in Malaysia*.
- [45] M.H.M Sabri, M. R. Ahmad etc (20 December 2020). *VHF Emissions Prior to Onset of Initial Electric Field Changes of Intracloud Flashes*. Retrieved from http://eprints.utm.my/id/eprint/88828/1/MohdRiduanAhmad2019_VHFEmissionsPriortotheOnsetofInitial.pdf
- [46] Mardina Abdullah, Siti Aminah Bahari (24 November 2020). *What Works Well (www) during Covid-19: Shifting to virtual*.
- [47] TWC Product and Technology LLC (2014). *Understanding Weather Radar*. Retrieved from <https://www.wunderground.com/prepare/understanding-radar>
- [48] ASCE (12 May 2018). *RADAR RAINFALL ESTIMATION*. Retrieved from ascelibrary.org by York University/Scott Library
- [49] Burgess, D.W. and Ray, P.S. (1986) Principles of the Radar. In: Ray, P., Ed., *Mesoscale Meteorology and Forecasting*, American Meteorological Society, Boston, 85-117.

